6-5-53 Copy No. 17

CONFIDENTIAL

RM No. A7A31

NACA

RESEARCH MEMORANDUM

DEVELOPMENT OF NACA SUBMERGED INLETS AND A COMPARISON WITH WING LEADING-EDGE INLETS FOR A $\frac{1}{4}$-SCALE MODEL OF A FIGHTER AIRPLANE

By Emmet A. Mossman and Donald E. Gault

Ames Aeronautical Laboratory
Moffett Field, Calif.

NATIONAL ADVISORY COMMITTEE
FOR AERONAUTICS

WASHINGTON
August 7, 1947

CONFIDENTIAL

NATIONAL ADVISORY COMMITTEE FOR AERONAUTICS

RESEARCH MEMORANDUM

DEVELOPMENT OF NACA SUBMERGED INLETS AND A COMPARISON WITH WING LEADING-EDGE INLETS FOR A 1/4-SCALE MODEL OF A FIGHTER AIRPLANE

By Emmet A. Mossman and Donald E. Gault

SUMMARY

Characteristics of NACA submerged duct entries and wing leading-edge inlets designed for a 1/4-scale flow model of a fighter-type airplane powered by a jet engine in the fuselage are presented. Duct total-head losses at the simulated entrance to the jet engine and pressure distributions over the duct entries are shown. A comparison of the dynamic pressure recovery and critical Mach number of the two intake systems is made. Included is a discussion of methods of ameliorating a duct-flow instability which may appear with a twin-entrance submerged duct system.

The dynamic pressure-recovery results indicate that, for a jet-propelled airplane with the jet engine in the fuselage, NACA submerged duct entries afford a better method of supplying air to the jet engine than wing leading-edge duct entries. This choice of the submerged entry is mainly due to the complex internal ducting of the wing leading-edge system. The critical Mach number is shown to be higher for these NACA submerged fuselage entries than for the basic wing section or the wing leading-edge duct entries, through the high-speed range down to 280 miles per hour (C_L=0.20), for sea level flight.

INTRODUCTION

Airplanes or missiles which utilize the oxygen of the atmosphere for combustion in their propulsive systems require that the air be ducted with a minimum pressure loss from the free stream to the entrance of the engine. Small losses in internal-flow systems handling the large quantities of air required by jet engines cause serious decreases in the thrust and appreciable increases in the fuel consumption so that the attainment of optimum performance from a jet-powered airplane depends, in great part, upon the selection and design of a ducting system which will supply air to the jet engine with maximum efficiency.

This report is concerned with the problem of obtaining maximum ducting efficiency for a jet-propelled airplane by partially converting the kinetic energy of the entering air to pressure energy, and conserving the remainder of the kinetic energy so that a minimum pressure loss results at the entrance to the jet-engine compressor. In this investigation two ducting systems of dissimilar geometry were designed and installed on a 1/4-scale flow model of a typical fighter airplane. One design incorporated NACA submerged inlets and the other, wing leading-edge inlets. Because the same model was used for the two duct installations and the air quantity requirements through the range of flight attitudes were identical for the two systems, this investigation afforded an excellent means of comparing their relative merits.

This work was done in the Ames 7- by 10-foot wind tunnel in conjunction with the general investigation of jet-motor air intakes being conducted at the various laboratories of the NACA. The design criteria for the NACA submerged ducts were taken from reference 1.

SYMBOLS

The symbols used throughout this report are defined as follows:

$C_{L_{airplane}}$	airplane lift coefficient
Δh	total-head loss in boundary layer
ΔH	loss in total-head of the duct system from free stream to the entrance of the jet engine
ΔH_E	loss in total-head from free stream to duct entrance
ΔH_D	loss in total-head from duct entrance to entrance to jet engine
P	pressure coefficient $[(p_l-p_o)/q_o]$
p_l	local static pressure
p_o	free-stream static pressure

q_e	dynamic pressure at duct entrance $\left(\frac{1}{2}\rho V_1^{\,2}\right)$
q_o	free-stream dynamic pressure $\left(\frac{1}{2}\rho V_o^{\,2}\right)$
V_1	duct-inlet velocity
V_o	free-stream velocity
V_1/V_o	inlet-velocity ratio
α	angle of attack referred to fuselage reference line degrees
ρ	mass density of air, slugs per cubic foot
η	total dynamic pressure recovery $\left(1 - \frac{\Delta H}{q_o}\right)$
η_E	dynamic pressure recovery at duct entrance $\left(1 - \frac{\Delta H_E}{q_o}\right)$
η_D	internal duct efficiency $\left(1 - \frac{\Delta H_D}{q_e}\right)$

MODEL AND APPARATUS

The 1/4-scale, partial-span, flow model of a fighter-type airplane used in these tests was originally designed as a model of a jet-boosted airplane. For this series of tests, however, it was assumed that the front reciprocating engine was removed and that the rear jet engine was the only means of propulsion. The jet-engine air-inlet systems were removable so that NACA submerged and wing leading-edge ducts could be tested alternately. The model, constructed of laminated mahogany over a steel framework, had no provisions for landing gear or empennage.

For the NACA submerged duct entry application, twin entrances, symmetrical about the longitudinal axis, were located along the sides of the fuselage 2 inches (model scale) forward of the junction of the wing leading edge and the fuselage. The air drawn through the submerged entrance was ducted directly aft, making one gradual turn inboard to the jet engine when clear of the pilot's enclosure. The wing leading-edge duct system, also symmetrical about the longitudinal axis, first ducted the air inboard from the wing leading edge ahead of the wing spar, next turned upward into the fuselage, and then parallel to the thrust axis with a final turn inboard to the entrance of the jet unit similar to that for the submerged entry. Each wing leading-edge duct made three approximately 45° turns in the horizontal plane and two 50° turns in the vertical plane. A comparison of the internal ducting of the NACA submerged duct entry and the wing leading-edge entry is presented in figures 1 and 2.

Full-scale wing and flap dimensions for the airplane are given in table I, while figure 3 presents a drawing of the airplane on which is indicated the wing span of this 1/4-scale flow model. The model, equipped with wing leading-edge ducts and flaps deflected 50°, is shown mounted in the tunnel in figure 4.

For bench tests to determine the duct efficiency, air was drawn through the left-hand ducts by a throttle-controlled constant-speed blower. (See fig. 5.) A plenum chamber and duct-exit turning vanes were used for these tests to duplicate, as closely as possible, the flow conditions of the wind-tunnel tests and to eliminate any effect of the butterfly-type throttle. Quantity flow was measured by a standard venturi located downstream of the plenum chamber. The duct total-head losses were measured at the simulated entrance to the jet motor by a rake consisting of 17 shielded total-head tubes connected to an integrating manometer and four static-head tubes.

For the wind-tunnel tests, the inlet air was drawn through the model by a centrifugal pump driven by a variable-speed electric motor. The air, after passing through the ducting systems, was discharged into a plenum chamber in the fuselage (fig. 6). From this chamber, the air was drawn out of the model through a duct in the wing spar and entered a mercury seal which isolated the wind-tunnel scale system from forces on the external ducting system. Quantity flow of air was measured by a standard orifice placed downstream from the mercury seal, the discharge end of the orifice leading to the pump located outside of the wind tunnel.

The total-head losses were measured by pressure-tube rakes, one placed in each duct at the simulated entrance to the jet motor. Both rakes were identical to the rake used for the separate tests on the internal ducting systems and were connected to a single integrating manometer to allow evaluation of the over-all losses. The pressure distributions were obtained from orifices built into the model and connected to liquid-in-glass manometers. All pressures were recorded photographically.

TEST METHODS

Prior to the tests necessary for a comparison between the two systems, a developmental investigation was made to devise an entrance configuration which gave the highest ram recovery over the flight range of inlet-velocity ratios from cruising to high speed. In this preliminary study the geometry of the ramp and deflectors were altered and a final configuration obtained from consideration of maximum pressure recovery. The model angle of attack was held constant ($\alpha=0^\circ$) and the inlet-velocity ratio varied throughout these tests.

At the conclusion of the developmental studies, total-head losses at the simulated entrance to the jet engine were measured for both duct systems. These losses were obtained throughout the angle-of-attack range for flaps retracted and flaps deflected 50° at inlet-velocity ratios of 0.20 to 3.00.

A method was devised relating the airplane lift coefficient with the flow model angle of attack. These relationships are given in figure 7 for flaps retracted and flaps deflected 50°. From this figure and the relationship between inlet-velocity ratio and airplane lift coefficient given in figure 8, the total-head losses can be found for all flight conditions.

In order to facilitate the model testing, a relationship was derived for setting inlet-velocity ratio by means of the orifice pressure drop. It was assumed in the derivation that the density at the duct entrance was the same as that in the free stream, which is true only at inlet-velocity ratios of 1.00. However, the error in inlet-velocity ratio was negligible, amounting to 0.2 of 1 percent and 2.0 percent at ratios equal to 0.20 and 3.00, respectively.

For the submerged duct installation, pressure distributions were taken along the center line of the lip and ramp for both constant angle of attack ($\alpha=0^\circ$) throughout the inflow range, and for matched conditions of $C_{L_{airplane}}$, model angle of attack, and inlet-velocity ratio that simulated flight at sea level. Pressure data for the wing leading-edge inlet were obtained throughout the angle-of-attack range for several inlet-velocity ratios that could be encountered in high-speed flight.

RESULTS AND DISCUSSION

Development of the Intake Systems

It was realized that in the application of the submerged duct criteria, the proximity of the wing to the duct entry and the curvature of the fuselage contour, factors which could not be evaluated in the general investigation, might modify the placement and exterior shape of the entrance for maximum dynamic-pressure recovery throughout the important flight range. A previous application of a submerged-duct system disclosed that, when the duct entry was placed adjacent to the wing, the flow field of the wing had an adverse effect on the lip-pressure distribution and induced a flow interference along the ramp. For these reasons, the entry was placed as far forward of the wing leading edge as possible. Preliminary tests were made to devise an entrance configuration giving the highest ram recovery over the flight range of inlet-velocity ratios from cruising to high speed.

Reference 1 states that the deflector size for submerged inlets is determined primarily by the boundary-layer thickness. Therefore, measurements were taken on the basic fuselage contour at the station corresponding to the lip of the submerged entry. The boundary-layer profile obtained, compared in figure 9 with boundary layer 1 of reference 1, indicated that the deflector size required would be similar to the small or normal deflectors. Using the entrance losses of reference 1 for an entrance configuration and boundary-layer thickness that closely approximated the conditions on this model, it was desired to estimate the total-head recovery that could be expected for the NACA submerged entry by the following relation:

$$\eta = \eta_E + (\eta_D - 1)(V_1/V_0)^2$$

This served as a guide to the preliminary studies in which the geometry of the ramp and deflectors were altered to obtain the highest recoveries through the important flight range.

Use of the aforementioned relationship required the determination of the duct efficiency from separate tests on the internal-ducting system. Bench tests conducted on the left-hand internal duct indicated a 92-percent duct efficiency (fig. 10). A tuft study disclosed no stall in the curved section of the duct, and it is believed that vanes would not improve the recovery.

A comparison of the estimated pressure recovery and that obtained with the final submerged-duct-entry configuration is shown in figure 11. Considering the presence of the wing and the fuselage-surface curvature (factors mentioned previously which were not evaluated in the general investigation of NACA submerged inlets), and, in addition, the probability of a slight change in duct efficiency with inlet-velocity ratio, it is thought that the estimated and actual total-head recoveries are in good agreement.

It should be emphasized that no drag evaluation was made in this or subsequent tests, and that the final duct-entrance configuration was determined only from considerations of the dynamic-pressure recovery and critical Mach number of the lip.

Views of the final submerged duct entrance configuration are presented in figures 12(a) and 12(b). Ordinates for the plan-form shape of the ramp and deflectors, and the lip-contour ordinates are presented in figure 13.

Separate tests were made on the wing leading-edge internal ducting to determine its efficiency. Several tests were made to obtain the best pressure recovery with various guide-vane configurations. The ducting efficiency obtained, 64 percent (fig. 10), indicates that the several bends, even with guide vanes, occasion considerable losses. The internal-structure arrangement of the wing and fuselage largely determines the complexity of the ducting system for wing leading-edge inlets. The usual result has been low internal-ducting efficiencies. If these internal-ducting efficiencies could be improved, major increases in the pressure recovery at the entrance to the jet-engine compressor would result. However, for the type of aircraft considered, with the jet engine in the fuselage and using wing leading-edge inlets, no significant gains have been found. With the tendency toward thinner wings on high-speed aircraft, and with the increased air requirements of the new high-thrust jet motors, it is probable that using wing inlets on this type airplane will become more difficult.

The wing leading-edge inlet is shown in figure 4. A comparison of the plain and ducted wing sections together with pertinent ordinates are given in figure 14.

Comparison of the Intake Systems

Dynamic-pressure losses.- Upon completion of preliminary tests and selection of the submerged-duct-entrance and wing leading-edge-inlet configurations, the duct total-head losses were determined.

Tables II and III present the pressure losses as a ratio of free-stream dynamic pressure for flaps retracted and flaps deflected 50°, respectively. The total-head losses as a function of airplane lift coefficient throughout the flight range, flaps retracted and flaps deflected 50°, were obtained from these data by cross-plotting for proper values of angle of attack and inlet-velocity ratio.

The total-head losses, flaps retracted, for NACA submerged and wing leading-edge duct systems are compared in figure 15 for sea-level and 30,000-foot operating conditions. On the same figure is presented the comparison for flaps deflected 50° at sea level. Examination of figure 16, which compares the dynamic-pressure recoveries for the two systems throughout the speed range, shows a greater pressure recovery for the NACA submerged duct entries for all flight conditions. Of particular interest is the high-pressure recovery over a wide range of flight speeds that is obtainable with the NACA submerged duct entries on this installation.

<u>Pressure distribution</u>.- Table IV lists in tabular form the pressure distribution in terms of pressure coefficients over the lip of the NACA submerged duct entry for constant angle of attack (α=0°) through the inflow range, and for matched flight conditions at sea level. Figures 17(a) and 17(b) present the pressure distribution along the bottom of the ramp for these same conditions. Because the ramp was lengthened while the model was in the tunnel, pressure tubes are lacking over the first 3 inches. This is unfortunate, since the pressures are still rising in this section. However, these pressures over the front portion of the ramp (fig. 17) are unduly high and not representative, since, for the submerged-duct installation, the velocity ratio of the air entering the cowl was zero, thereby causing high pressure peaks over the forward portion of the cowling. A streamline nose shape would provide a more favorable pressure gradient on this front portion of the ramp.

Pressure distribution for the wing leading-edge inlet is tabulated in tables V to XI for the wing-fuselage juncture with the plain and ducted wing section and the outboard closing shape (wing station 18, fig. 14.) For all practical purposes, the pressure distribution at the wing-fuselage juncture and outboard closing shape was found to be independent of inlet-velocity ratio.

The critical Mach numbers were determined from the peak negative pressure coefficients of the two systems by the Kármán-Tsien method outlined in reference 2. The critical Mach numbers for matched conditions at sea level for NACA submerged and wing leading-edge inlets are shown in figure 18. Included is a comparison of the critical Mach number of the two inlets, which shows the NACA submerged duct entry to be higher through the range of high speed down to 280 miles per hour (C_L=0.20) for sea-level flight. In the high-speed attitude the comparative values are 0.75 for the NACA submerged inlet and 0.67 for the wing leading-edge inlet. Although sufficient data are not available for a direct comparison at altitude, the use of NACA submerged ducts for this installation should prove more advantageous through a comparable speed range. In comparing the two type inlets at some other altitude for a given flight condition, the change in the critical Mach number characteristics from those shown on figure 18 would be due, primarily, to change in angle of attack. The wing leading-edge inlet is more sensitive in this respect, so that the difference between the two entries as shown on figure 18 should be accentuated. The effect of the change in inlet-velocity ratio with altitude for a given flight condition is of secondary importance. Pressure distributions were not measured over the deflectors. In this series of tests the deflectors were developed solely from the standpoint of increased pressure recovery at the entrance of the inlet. The existing deflector configuration should not be considered as final, and it is probable that more gradual contours could be utilized for more favorable air flow along the fuselage.

It should be emphasized that the critical Mach number of the submerged duct entry is to a large extent dependent upon the type of pressure field in which the duct is placed. A location nearer the wing will give somewhat lower critical Mach numbers.

Flow instability in a twin NACA submerged duct system.- Under certain flow conditions at low inlet-velocity ratios, an unstable condition of the entering air may be encountered with a twin NACA submerged duct system. This instability is common to ducting systems consiting of two entrance channels which discharge into a common reservoir, provided that, with increasing inlet-velocity ratio, the total-head losses first decrease and then increase. This condition can exist, as in this case, where the entering flow is constrained on one or more sides so that some boundary-layer air is taken in.

Whether the instability would occur in the actual installation depends upon the mechanical design of the jet motor. If the air empties into a common chamber before entering the jet-motor compressor, the instability could occur.

At present the inlet-velocity ratio at the start of instability cannot be predicted, but it has been observed that instability never occurs at ratios above that at maximum recovery. In order to prevent instability the entrance ducts should be designed for a high-speed inlet-velocity ratio that allows a margin of 0.2 to 0.3 above that at instability. This would permit the jet motor to be throttled considerably and still operate in the stable range. However, if this does not allow for sufficient throttling, then mechanical devices could be used which would either maintain inlet-velocity ratios above that at instability when the engine was throttled, or would decrease the ram recovery so that the maximum recovery would occur at inlet-velocity ratios below those at which the airplane was momentarily operating.

The bottom of the ramp could be hinged at the forward end so that the inlet area could be reduced or completely closed off by a trap-door arrangement. This would not only eliminate the instability but also enable a jet-boosted aircraft, cruising with the jet motor inoperative, to eliminate the high drag due to air bleeding through the jet motor. For use in a completely jet-propelled airplane, a butterfly valve in one of the entrance channels could be automatically moved in conjunction with the throttle, so that when the speed of the jet motor was reduced below a certain value, the valve would be actuated enough to eliminate the instability. Another possible means of ameliorating this condition is the provision of a hatch in the ducting system, forward of the compressor, which could be opened when the jet motor is throttled back to allow air to bleed to the free stream. This would permit continued operation in the noncritical inlet-velocity-ratio range, and control could be made similar to the aforementioned butterfly valve. This last method of bleeding air through the duct and the first method using the flexible ramp would also eliminate the low critical Mach numbers that result from high negative pressures over the outside of the lip at low inlet-velocity ratios. A further advantage of any of these mechanical devices is that they also would facilitate starting the jet-engine in high-speed flight by lowering the air velocity through the combustion chamber to that necessary for flame propagation.

In the consideration or selection of instability-eliminating devices such as those described, it is of prime importance that the device should cause no decrease in ram when not in use. When the device is in use, however, any loss in ram resulting from its operation will be of minor importance, since the unstable regime usually occurs with the airplane at high speed and the jet motor throttled.

If the ducting could be so designed that a single NACA submerged entrance would lead to a single jet engine, this instability would not occur. For a jet installation on a swept-back wing, where the use of nacelles for the jet engines incurs a premature drag rise (reference 3), this principle might be applied advantageously by locating the jet engines in the fuselage.

CONCLUSIONS

From this experimental investigation of an NACA submerged duct installation and the comparison with wing leading-edge inlets it is concluded that:

1. For a completely jet-propelled aircraft with the jet engine in the fuselage, NACA submerged entries merit serious consideration as a means of supplying air to the jet engine. For this installation, NACA submerged duct entries gave higher pressure recoveries at the entrance to the jet engine than wing leading-edge inlets throughout the flight speed range.

2. The critical Mach number (0.75) of this NACA submerged duct is greater than that of the basic wing sections used on present-day fighters.

3. For this type installation (a jet-propelled airplane with jet engine in the fuselage) the complexity of the duct and airplane structural design would be greatly reduced by using an NACA submerged-duct entry.

4. A flow instability in the ducting system, which would not occur with wing leading-edge duct entries, could exist at low inlet-velocity ratios with twin NACA submerged air inlets. By proper selection of the high-speed inlet-velocity ratio, this condition could be precluded from ordinary flight. For high-speed-flight attitudes with the jet engine throttled, mechanical methods of alleviating the instability should be employed.

Ames Aeronautical Laboratory,
National Advisory Committee for Aeronautics,
Moffett Field, Calif.

REFERENCES

1. Frick, Charles W., Davis, Wallace F., Randall, Lauros M., and Mossman, Emmet A.: An Experimental Investigation of NACA Submerged-Duct Entrances. NACA ACR No. 5I20, 1945.

2. von Kármán, Th.: Compressibility Effects in Aerodynamics. Jour. Aero. Sci., vol. 8, no. 9, July 1941, pp. 337-356.

3. H. Ludweig: Pheilflugel bei hohen Goschwindigkeiten (Swept-back Wings at High Velocities). Rep. No. 127 Lilienthal-Geselschaft fur Luftfahrtforschung. Sept. 1940.

TABLE I.- FULL-SCALE GEOMETRIC WING AND FLAPS CHARACTERISTICS FOR THE FIGHTER AIRPLANE

~~CONFIDENTIAL~~

Wing	
Area, sq ft	400.25
Span, ft	48.00
M.A.C., in.	104.6
Root chord, in.	140
Tip chord, in.	60
Root section	66(215)-214-1.0
Tip section	65(112)-213-1.0
Geometric twist, deg	$2\frac{1}{2}$
Aspect ratio	5.76
Taper ratio	2.33
Incidence at root chord, deg	1
Dihedral of chord plane, deg	$6\frac{1}{2}$
Flaps	
Total area, sq ft	50.8
Over-all span, ft	22.56
Chord	23 percent wing chord
Travel, deg	0 to 50
Wing area affected, sq ft	221.6
Type	Extensible-slotted, with fixed vane on leading edge and operating on fixed tracks

~~CONFIDENTIAL~~

NATIONAL ADVISORY COMMITTEE FOR AERONAUTICS

TABLE II.- DUCT TOTAL HEAD LOSSES MEASURED AT THE SIMULATED ENTRANCE TO THE JET-ENGINE FOR THE 1/4-SCALE FLOW MODEL OF THE FIGHTER AIRPLANE WITH FLAPS RETRACTED

CONFIDENTIAL

NACA submerged ducts																
$\frac{V_1}{V_0}$ \ α	-3.04	-2.02	-1.01	0	1.02	2.05	3.06	4.07	5.08	6.10	7.11	8.13	9.14	10.14	11.14	12.13
0.2	0.220[a]	0.210	0.189	0.183	0.210	0.173	0.183	0.215	0.253	0.281	0.309	0.330	0.343	0.357	0.358	0.355
.3	.193	.178	.157	.147	.157	.168	.189	.204	.228	.252	.262	.279	.295	.314	.309	---
.4	.157	.142	.126	.122	.122	.136	.153	.169	.188	.191	.200	.211	.226	.237	.261	.252
.5	.126	.120	.105	.095	.095	.100	.115	.131	.138	.138	.143	.157	.168	.179	.189	.189
.6	.110	.111	.100	.079	.074	.085	.090	.100	.105	.110	.110	.121	.127	.132	.144	.147
.7	.110	.100	.090	.079	.067	.073	.079	.085	.090	.094	.104	.110	.115	.119	.124	.130
.8	.121	.105	.095	.079	.069	.074	.079	.084	.090	.094	.104	.116	.121	.120	.133	.139
1.0	.163	.157	.137	.117	.104	.095	.094	.100	.106	.116	.121	.132	.142	.158	.247	.261
1.2	.201	.192	.172	.142	.136	.136	.130	.130	.145	.159	.173	.183	.192	.268	.302	.320
1.4	.286	.282	.264	.219	.240	.230	.225	.235	.238	.264	.277	.292	.299	.324	.373	.403
2.0	.524	.556	.556	.556	.546	.546	.513	.513	.513	.546	.546	.568	.600	.618	.680	.680
2.2	.622	.618	.666	.666	.618	.666	.666	.666	.666	.666	.687	.722	.708	.736	.816	.819
2.5	.652	.694	.715	.736	.762	.782	.782	.782	.799	.841	.858	.820	.840	.882	.883	.966
3.0	.909	.999	1.063	1.060	1.090	1.121	1.186	1.218	1.249	1.242	1.303	1.273	1.303	1.324	1.324	1.393
Wing leading-edge ducts																
$\frac{V_1}{V_0}$ \ α	-3.04	-2.02	-1.01	0	1.02	2.05	3.06	4.07	5.08	6.10	7.11	8.13	9.14	10.14	11.14	12.13
0.21	0.439[a]	0.233	0.145	0.082	0.068	0.062	0.063	0.057	0.063	0.080	0.096	0.130	0.167	0.159	0.136	0.132
.43	.423	.299	.167	.125	.105	.111	.111	.111	.133	.145	.181	.216	.271	.317	.243	.224
.65	.494	.330	.205	.182	.182	.184	.187	.198	.221	.259	.293	.364	.441	.519	.494	.515
.87	.536	.358	.242	.252	.249	.261	.283	.306	.351	.383	.448	.501	.591	.706	.744	.570
1.08	.631	.407	.355	.362	.381	.390	.411	.443	.491	.546	.620	.673	.858	.909	.988	.890
1.30	.660	.455	.443	.456	.470	.494	.515	.556	.603	.685	.754	.858	.962	1.058	1.139	1.051
1.52	.685	.598	.589	.598	.596	.644	.685	.727	.808	.877	.977	1.077	1.178	1.328	1.395	1.345
2.17	1.314	1.261	1.261	1.332	1.408	1.462	1.524	1.622	1.729	1.854	1.996	2.200	2.300	2.389	2.440	2.440

[a]Value based on free-stream dynamic pressure $\Delta H/q_0$.

CONFIDENTIAL

NATIONAL ADVISORY
COMMITTEE FOR AERONAUTICS

TABLE III.- DUCT TOTAL-HEAD LOSSES, MEASURED AT THE SIMULATED ENTRANCE TO THE JET-ENGINE, FOR THE 1/4-SCALE FLOW MODEL OF THE FIGHTER AIRPLANE WITH FLAPS DEFLECTED 50°

CONFIDENTIAL

NACA submerged ducts

$\frac{V_1}{V_0}$ \ α	-8.05	-7.03	-6.01	-5.0	-3.99	-2.97	-1.95	-0.94	0.08	1.10	2.12	3.12	4.12	5.13
0.2	0.297[a]	0.198	0.172	0.193	0.193	0.178	0.194	0.227	0.266	0.303	0.330	0.348	0.378	0.360
.3	.238	.188	.168	.168	.167	192	.203	.231	.250	.282	.308	.320	.325	.339
.4	.193	.173	.145	.139	.145	.157	.172	.197	.214	.223	.245	.247	.265	.256
.5	.150	.136	.120	.121	.121	.126	.142	.157	.169	.178	.189	.188	.194	.200
.6	.126	.115	.105	.101	.100	.100	.110	.119	.132	.137	.136	.137	.142	.148
.7	.121	.111	.111	.091	.090	.085	.095	.100	.111	.115	.122	.119	.125	.126
.8	.122	.111	.100	.091	.086	.085	.085	.093	.105	.111	.114	.119	.125	.126
1.0	.145	.136	.125	.115	.111	.106	.105	.111	.116	.126	.132	.142	.142	.142
1.2	.192	.191	.174	.158	.147	.138	.133	.143	.154	.164	.165	.170	.175	.186
1.4	.285	.271	.253	.242	.232	.232	.253	.238	.238	.248	.261	.282	.292	.294
2.0	.537	.558	.592	.614	.601	.601	.580	.570	.558	.558	.548	.546	.558	.580
2.2	.622	.610	.618	.652	.673	.708	.639	.652	.673	.673	.639	.618	.639	.673
2.5	.694	.673	.715	.736	.795	.816	.799	.837	.837	.820	.841	.841	.841	.841
3.0	.883	.912	.942	1.030	1.059	1.090	1.090	1.118	1.178	1.207	1.207	1.207	1.265	1.265

Wing leading-edge ducts

$\frac{V_1}{V_0}$ \ α	-8.05	-7.03	-6.01	-5.00	-3.99	-2.97	-1.95	-0.94	0.08	1.10	2.12	3.12	4.12	5.13
0.21	0.094	0.068	0.055	0.055	0.054	0.055	0.070	0.082	0.118	0.169	0.206	0.244	0.220	0.218
.43	.136	.110	.103	.104	.111	.119	.149	.161	.220	.291	.366	.401	.408	.386
.65	.180	.165	.168	.168	.189	.209	.234	.282	.359	.434	.505	.505	.522	.558
.87	.234	.249	.259	.271	.295	.332	.366	.435	.512	.616	.722	.855	.857	.828
1.08	.350	.352	.364	.388	.429	.461	.540	.602	.696	.790	.940	1.063	.963	1.029
1.30	.466	.477	.494	.508	.546	.602	.670	.755	.839	.968	1.106	1.156	1.318	1.238
1.52	.598	.597	.627	.674	.704	.771	.860	.968	1.079	1.190	1.346	1.356	1.456	1.467
2.17	1.255	1.221	1.355	1.344	1.445	1.498	1.567	1.671	1.809	1.929	2.032	2.170	2.362	2.400

[a]Value based on free-stream dynamic pressure $\Delta H/q_0$.

CONFIDENTIAL

NATIONAL ADVISORY COMMITTEE FOR AERONAUTICS

~~CONFIDENTIAL~~

TABLE IV.- PRESSURE DISTRIBUTION OVER THE LIP OF THE SUBMERGED DUCT ENTRY FOR THE 1/4-SCALE FLOW MODEL OF THE FIGHTER AIRPLANE

Matched conditions at sea level, propeller removed														
Distance from lip L.E. (in.)		1.47	0.84	0.53	0.21	0.06	0	0.06	0.21	0.84	1.47	2.09	4.59	5.84
V_i/V_o	α \ P	Inside						Outside						
0.54	-0.5	0.529	0.504	0.534	0.683	0.913	0.703	0.035	-0.359	-0.419	-0.334	-0.259	-0.065	-0.090
.75	-.1	.234	.188	.198	.254	.519	.978	.112	-.173	-.316	-.290	-.249	-.087	-.112
.80	0	.153	.092	.097	.127	.382	.987	.249	-.122	-.285	-.280	-.244	-.087	-.117
1.00	.5	-.241	-.371	-.391	-.482	-.431	.841	.641	-.070	-.201	-.241	-.221	-.110	-.130
1.20	1.2	-.672	-.853	-.933	-1.193	-1.445	.722	.833	.070	-.181	-.241	-.261	-.171	-.191
1.40	1.9	-1.093	-1.223	1.440	-1.917	-2.533	.318	. 26	.170	-.119	-.239	-.278	-.209	-.229
1.60	2.8	-1.745	-2.039	-2.233	-3.039	-4.350	-.647	[illegible]	.230	-.020	-.196	-.235	-.216	-.288
2.00	4.8	-2.980	-3.470	-3.823	-5.195	-8.160	-2.941	.882	.177	.020	-.216	-.333	-.333	-.353
2.20	6.0	-3.720	-4.240	-4.800	-6.620	-10.540	-4.740	.720	.140	0	-.280	-.440	-.460	-.480
α = 0°														
V_i/V_o	α \ P	Inside						Outside						
0.41	0	0.622	0.606	0.653	0.334	0.999	0.434	-0.890	-0.449	-0.519	-0.392	-0.310	-0.108	-0.137
.44	0	.636	.590	.636	.812	.986	.499	-.802	-.467	-.502	-.388	-.304	-.105	-.137
.47	0	.582	.562	.602	.771	.967	.578	-.683	-.460	-.487	-.379	-.304	-.108	-.140
.52	0	.550	.529	.570	.729	.945	.647	-.582	-.460	-.476	-.379	-.305	.110	-.138
.56	0	.491	.460	.496	.636	.894	.791	-.398	-.398	-.445	-.367	-.300	-.109	-.150
.62	0	.428	.393	.422	.544	.810	.850	-.260	-.318	-.399	-.347	-.284	-.098	-.127
.66	0	.355	.315	.342	.429	.704	.911	-.107	-.268	-.369	-.322	-.275	-.101	-.127
.73	0	.257	.209	.225	.289	.554	.972	.072	-.241	-.321	-.297	-.265	-.096	-.121
.81	0	.091	.030	.030	.040	.334	.980	.323	-.131	-.283	-.283	-.253	-.091	-.121
.94	0	-.147	-.254	-.267	-.320	-.214	.947	.547	-.067	-.214	-.240	-.227	-.107	-.120
1.16	0	-.840	-.820	-.860	-1.120	-1.300	.680	.820	0	-.080	-.140	-.160	-.060	-.080
1.48	0	-1.548	-1.808	-1.968	-2.483	-3.450	-.323	.968	.194	.065	-.032	-.065	-.032	-.032
1.81	0	2.572	-3.048	-3.142	-4.478	-6.140	-1.999	1 000	.333	.190	.048	0	0	0
2.17	0	-4.068	-4.668	-4.933	-7.265	-9.580	-4.532	.734	.333	.267	.133	0	0	0
2.56	0	-7.55	-8.44	-9.22	-15.23	-16.[illegible]	-10.22	0	.111	.444	.222	0	0	0

~~CONFIDENTIAL~~

NATIONAL ADVISORY COMMITTEE FOR AERONAUTICS

TABLE V.-WING FUSELAGE-JUNCTURE PRESSURE DISTRIBUTION (WITHOUT WING LEADING-EDGE DUCT ENTRIES INSTALLED) FOR THE 1/4-SCALE FLOW MODEL OF THE FIGHTER AIRPLANE

~~CONFIDENTIAL~~

% chord \ α	P									
	-4.05	-2.02	-1.01	0	1.02	2.05	4.07	6.10	8.13	10.14
Upper surface										
0	-0.574	-0.088	0.166	0.346	0.490	0.617	0.696	0.604	0.423	0.186
1.0	.749	.868	.720	.498	.204	-.120	-.826	-1.814	-2.770	-3.901
2.5	.367	.135	.071	.048	.008	.024	-.996	-1.875	-2.300	-2.990
5.0	.526	.223	.055	-.145	-.383	-.617	-1.077	-1.625	-2.090	-3.622
7.0	.303	.040	-.127	-.305	-.514	-.689	-1.053	-1.495	-1.860	-2.268
10	.231	-.096	-.253	-.418	-.604	-.745	-1.044	-1.421	-1.718	-2.032
15	-.008	-.287	-.434	-.570	-.718	-.745	-1.069	-1.347	-1.552	-1.773
19	-.167	-.398	-.522	-.643	-.776	-.857	-1.061	-1.282	-1.436	-1.586
29	-.295	-.446	-.545	-.627	-.726	-.777	-.907	-1.045	-1.128	-1.190
40	-.398	-.510	-.585	-.658	-.726	-.753	-.858	-.956	-.980	-.988
53	-.446	-.510	-.569	-.618	-.670	-.681	-.736	-.776	-.730	-.656
60	-.391	-.414	-.443	-.474	-.498	-.489	-.486	-.466	-.407	-.397
70	-.446	-.494	-.538	-.586	-.621	-.617	-.648	-.662	-.573	-.510
Lower surface										
1.0	-1.474	-.908	-.609	-.305	-.041	.216	.551	.816	.938	.980
2.5	-.956	-.598	-.419	-.233	-.073	.104	.348	.572	.738	.850
5.0	-.709	-.430	-.340	-.217	-.106	.024	.202	.392	.537	.656
7.5	-.646	-.358	-.340	-.241	-.155	-.040	.113	.278	.415	.526
10	-.622	-.422	-.348	-.257	-.188	-.080	.049	.204	.332	.445
15	-.566	-.407	-.348	-.289	-.229	-.144	-.032	.098	.216	.316
20	-.526	-.391	-.340	-.297	-.245	-.168	-.073	.033	.141	.218
30	-.430	-.335	-.301	-.257	-.216	-.152	-.113	-.016	.066	.121
40	-.414	-.335	-.308	-.273	-.253	-.184	-.146	-.082	-.008	.032
50	-.422	-.367	-.340	-.321	-.294	-.240	-.211	-.155	-.100	-.065
60	-.422	-.382	-.372	-.361	-.343	-.296	-.275	-.237	-.183	-.162
70	-.255	-.231	-.222	-.127	-.216	.176	-.178	-.155	-.125	-.113

~~CONFIDENTIAL~~

NATIONAL ADVISORY
COMMITTEE FOR AERONAUTICS

TABLE VI.-WING FUSELAGE-JUNCTURE PRESSURE DISTRIBUTION (WITH WING LEADING-EDGE DUCT ENTRIES INSTALLED) FOR THE 1/4-SCALE FLOW MODEL OF THE FIGHTER AIRPLANE

~~CONFIDENTIAL~~

% chord \ α	P									
	-3.04	-2.02	-1.01	0	1.02	2.05	4.07	6.10	8.13	10.14
Upper surface										
0	-0.337	0.037	0.306	0.540	0.754	0.864	0.991	0.998	0.924	0.202
1.0	.819	.730	.550	.290	-.007	-.321	-1.105	-2.083	-3.130	-2.910
2.5	.392	.295	-.095	-.162	-.448	-.710	-1.381	-2.228	-3.040	-2.750
5.0	.172	.034	-.156	-.371	-.624	-.851	-1.381	-1.968	-2.551	-2.480
7.0	.034	-.134	-.306	-.486	-.692	-.884	-1.273	-1.736	-2.171	-2.369
10	.021	-.214	-.374	-.512	-.686	-.831	-1.146	-1.510	-1.846	-2.248
15	-1.287	-.448	-.578	-.695	-.822	-.931	-1.166	-1.435	-1.615	-1.849
19	-.289	-.402	-.503	-.600	-.706	-.790	-.978	-1.183	-1.330	-1.457
29	-.275	-.342	-.401	-.479	-.550	-.616	-.724	-.861	-.971	-1.105
40	-.406	-.463	-.523	-.574	-.632	-.670	-.750	-.840	-.890	-.810
53	-.489	-.516	-.577	-.600	-.638	-.656	-.696	-.724	-.720	-.568
60	-.420	-.428	-.455	-.459	-.468	-.456	-.456	-.431	-.380	-.405
70	.007	0	-.007	.007	.007	.013	.007	.007	.007	.007
Lower surface										
1	-1.287	-.918	-.570	-.243	.041	.235	.603	.854	.964	.297
2.5	-.846	-.656	-.435	-.229	-.054	.080	.348	.574	.733	.844
5.0	-.598	-.448	-.333	-.196	-.075	.013	.228	.403	.544	.607
7.5	-.626	-.523	-.401	-.290	-.190	-.107	.080	.246	.387	.445
10	-.516	-.422	-.333	-.277	-.183	-.107	.054	.205	.340	.392
15	-.530	-.448	-.374	-.290	-.224	-.161	-.027	.096	.217	.256
20	-.489	-.428	-.360	-.290	-.231	-.188	-.060	.041	.149	.189
30	-.365	-.315	-.272	-.196	-.177	-.146	-.080	0	.082	.122
40	-.365	-.328	-.299	-.243	-.211	-.174	-.107	-.041	.027	.047
50	-.392	-.362	-.340	-.304	-.278	-.241	-.188	-.130	-.075	-.054
60	-.413	-.389	-.387	-.344	-.353	-.308	-.268	-.150	-.177	-.162
70	-.241	-.235	-.231	-.209	-.197	-.181	-.147	-.130	-.109	-.108

~~CONFIDENTIAL~~

NATIONAL ADVISORY
COMMITTEE FOR AERONAUTICS

TABLE VII.- PLAIN-WING PRESSURE DISTRIBUTION AT STATION 13.50, 1/4-SCALE FLOW MODEL OF THE FIGHTER AIRPLANE

~~CONFIDENTIAL~~

% chord \ α	P									
	-4.05	-2.02	-1.01	0	1.02	2.05	4.07	6.10	8.13	10.14
Upper surface										
0	0.303	0.344	0.972	0.980	0.906	0.715	0.130	-0.964	-2.258	-3.838
1.0	.313	.470	.205	-.129	-.506	-.908	-1.741	-2.825	-3.885	-5.310
2.5	.558	.255	.063	-.177	-.424	-.689	-1.263	-1.560	-2.190	-2.858
5.0	.239	.064	-.111	-.289	-.490	-.673	-.972	-1.437	-1.318	-2.250
7.5	.159	-.064	-.292	-.370	-.538	-.689	-.980	-1.356	-1.660	-2.008
10	.048	-.159	-.301	-.442	-.596	-.729	-.964	-1.290	-1.544	-1.821
15	-.064	-.255	-.364	-.498	-.620	-.721	-.915	-1.168	-1.361	-1.562
20	-.183	-.351	-.478	-.563	-.686	-.753	-.931	-1.143	-1.295	-1.441
30	-.287	-.414	-.498	-.595	-.678	-.721	-.850	-.980	-1.071	-1.150
40	-.375	-.470	-.538	-.611	-.686	-.715	-.810	-.906	-.946	-.955
50	-.446	-.534	-.577	-.635	-.694	-.715	-.770	-.825	-.822	-.769
60	-.494	-.558	-.593	-.659	-.686	-.697	-.704	-.727	-.672	-.558
70	-.422	-.494	-.514	-.530	-.530	-.529	-.513	-.490	-.415	-.389
Lower surface										
1.0	-1.785	-.860	-.458	-.113	.188	.441	.769	.956	.971	.390
2.5	-1.036	-.638	-.396	-.177	.024	.216	.486	.719	.872	.939
5.0	-.916	-.542	-.379	-.386	-.082	.072	.292	.506	.664	.777
7.5	-.789	-.502	-.379	-.257	-.131	-.008	.186	.368	.523	.632
10	-.662	-.446	-.340	-.241	-.136	-.016	.138	.294	.432	.551
15	-.582	-.430	-.356	-.273	-.196	-.096	.032	.171	.290	.397
20	-.590	-.438	-.364	-.313	-.253	-.160	-.040	.082	.174	.275
30	-.470	-.367	-.332	-.289	-.245	-.176	-.105	-.016	-.755	.146
40	-.438	-.383	-.332	-.305	-.269	-.208	-.154	-.082	-.008	-.040
50	-.446	-.383	-.364	-.338	-.310	-.264	-.219	-.163	-.108	-.057
60	-.438	-.398	-.372	-.354	-.335	-.296	-.267	-.228	-.183	-.146
70	-.263	-.239	-.237	-.273	-.253	-.208	-.186	-.163	-.133	-.113

~~CONFIDENTIAL~~

NATIONAL ADVISORY COMMITTEE FOR AERONAUTICS

CONFIDENTIAL

TABLE VIII.- PRESSURE DISTRIBUTION OVER THE WING LEADING-EDGE DUCT ENTRANCE, 1/4-SCALE FLOW MODEL OF THE FIGHTER AIRPLANE

$[V_1/V_0 = 0]$

% chord \ α	P								
	-3.04	-2.02	-1.01	1.02	2.05	4.07	6.10	8.13	10.14
Upper Surface									
0	0.978	0.818	0.493	-0.797	-1.745	-4.703	-5.889	-5.930	-3.022
1.0	.313	.073	-.236	-1.011	-1.456	-2.364	-3.546	-4.730	-2.057
2.5	.100	-.080	-.323	-.877	-1.160	-1.824	-2.569	-3.283	-2.042
5.0	-.120	-.266	-.459	-.850	-1.072	-1.505	-1.984	-2.432	-2.168
7.5	-.153	-.273	-.425	-.730	-.889	-1.218	-1.584	-1.914	-2.266
10	-----	-----	-----	------	------	------	------	------	------
15	-.206	-.286	-.385	-.596	-.708	-.912	-1.135	-1.335	-2.030
20	-.253	-.326	-.411	-.529	-.640	-.812	-.998	-1.150	-1.557
30	-.339	-.399	-.459	-.562	-.634	-.759	-.883	-.978	-.900
40	-.406	-.446	-.499	-.576	-.626	-.712	-.808	-.792	-.690
50	-.486	-.519	-.560	-.622	-.667	-.718	-.774	-.806	-.584
60	-.526	-.559	-.512	-.622	-.654	-.678	-.700	-.711	-.518
70	-.459	-.486	-.587	-.482	-.485	-.486	-.475	-.471	-.447
Upper Inner Surface									
1	.186	.186	.196	.221	-.452	.226	.910	.232	.860
2.5	.726	.812	.890	.958	.977	.992	.999	.998	.998
5	.726	.825	.890	.944	.977	.978	.979	.984	.985
Lower Inner Surface									
4.2	.672	.798	.884	.978	.991	.985	.965	.936	.939
5.7	.712	.818	.890	.951	.964	.952	.938	.930	.939
Lower Surface									
3.2	-1.171	-1.024	-2.090	-.670	-.067	.679	.938	.958	.946
4.2	-2.017	-1.679	-1.342	-.610	-.303	.186	.544	.786	.788
5.7	-1.517	-1.272	-1.031	-.529	-.310	.067	.367	.602	.624
8.2	-1.111	-.946	-.796	-.449	-.290	-.027	.285	.417	.447
10.7	-.852	-.726	-.600	-.342	-.222	-.013	.177	.342	.374
13.2	-.698	-.606	-.499	-.288	-.196	.013	.150	.294	.329
18.2	-.552	-.486	-.405	-.241	-.169	-.027	.109	.225	.263
23.2	-.499	-.439	-.378	-.241	-.182	-.053	.054	.158	.197
33.2	-.432	-.393	-.344	-.248	-.202	-.113	-.027	.055	.074
43.2	-.399	-.366	-.331	-.248	-.216	-.146	-.075	-.007	.013
53.2	-.413	-.379	-.351	-.281	-.256	-.193	-.136	-.075	-.066
63.2	-.413	-.393	-.364	-.322	-.303	-.260	-.211	-.157	-.164
73.2	-.246	-.240	-.223	-.194	-.182	-.153	-.129	-.103	-.125

CONFIDENTIAL

NATIONAL ADVISORY COMMITTEE FOR AERONAUTICS

CONFIDENTIAL

TABLE IX.– PRESSURE DISTRIBUTION OVER THE WING LEADING-EDGE DUCT ENTRANCE, 1/4-SCALE FLOW MODEL OF THE FIGHTER AIRPLANE

[V_1/V_0 = 0.2]

% Chord \ α	-3.04	-2.02	-1.01	0	1.02	2.05	4.07	6.10	8.13	10.14
	P									
Upper Surface										
0	0.990	0.966	0.768	0.337	-.353	-1.152	-3.339	-5.988	-5.950	-3.320
1.0	.441	-.187	-.109	-.452	-.882	-1.319	-2.158	-3.309	-4.480	-2.159
2.5	.193	-.013	-.251	-.512	-.828	-1.071	-1.675	-2.432	-3.160	-2.240
5.0	-.069	-.228	-.414	-.600	-.822	-1.018	-1.449	-1.920	-2.380	-2.390
7.5	-.117	-.248	-.401	-.540	-.720	-.851	-1.166	-1.531	-1.875	-2.429
10	----	----	----	----	----	----	----	----	----	----
15	-.186	-.281	-.387	-.486	-.598	-.690	-.884	-1.114	-1.318	-1.869
20	-.241	-.315	-.407	-.499	-.530	-.616	-.784	-.977	-1.135	-1.410
30	-.330	-.389	-.462	-.526	-.564	-.623	-.744	-.868	-.972	-.910
40	-.392	-.435	-.509	-.553	-.578	-.623	-.703	-.786	-.850	-.736
50	-.432	-.516	-.564	-.594	-.625	-.656	-.717	-.766	-.794	-.628
60	-.523	-.550	-.591	-.614	-.632	-.650	-.670	-.690	-.672	-.520
70	-.454	-.476	-.509	-.520	-.482	-.489	-.482	-.458	-.415	-.412
Upper Inner Surface										
1	.117	.127	.156	.161	.177	.181	.181	.178	.176	.135
2.5	.317	.502	.632	.769	.856	.904	.951	.984	.998	.978
5	.351	.562	.848	.897	.916	.924	.938	.950	.930	.910
Lower Surface										
3.2	-.151	-.134	-.081	.223	.530	.736	.972	.956	.714	.532
4.2	1.562	-1.220	-.916	-.600	-.326	-.080	.335	.670	.882	.890
5.7	1.321	-1.220	-.828	-.587	-.380	-.187	.147	.444	.666	.702
8.2	1.032	-.858	-.686	-.512	-.374	-.241	.020	.260	.455	.499
10.7	-.798	-.670	-.544	-.405	-.299	-.201	.007	.205	.367	.405
13.2	-.681	-.563	-.475	-.364	-.265	-.161	.007	.171	.306	.371
18.2	-.544	-.462	-.387	-.304	-.224	-.147	-.013	.116	.238	.290
23.2	-.495	-.429	-.374	-.297	-.224	-.161	-.047	.062	.170	216
33.2	-.434	-.332	-.340	-.290	-.238	-.194	-.114	-.027	.054	.088
43.2	-.399	-.362	-.319	-.283	-.245	-.208	-.141	-.075	-.007	.020
53.2	-.413	-.382	-.353	-.317	-.279	-.248	-.194	-.137	-.075	-.061
63.2	-.413	-.389	-.380	-.344	-.319	-.302	-.261	-.205	-.163	-.155
73.2	-.255	-.235	-.232	-.202	-.190	-.181	-.181	-.144	-.115	-.115
Lower Inner Surface										
4.2	.716	.844	.936	.951	.950	.938	.924	.902	.652	.594
5.7	.564	.737	.869	.890	.396	.904	.898	.888	.810	.762

CONFIDENTIAL

NATIONAL ADVISORY COMMITTEE FOR AERONAUTICS

CONFIDENTIAL

TABLE X.- PRESSURE DISTRIBUTION OVER THE WING LEADING-EDGE DUCT ENTRANCE, 1/4-SCALE FLOW MODEL OF THE FIGHTER AIRPLANE

[$V_1/V_0 = 0.4$]

	P									
% chord \ a	-3.04	-2.02	-1.01	0	1.02	2.05	4.07	6.10	8.13	10.14
Upper Surface										
0	0.972	0.986	0.844	0.509	-0.094	-0.864	-2.956	-7.065	------	-3.800
1.0	.486	.260	-.067	-.388	-.796	-1.220	-2.063	-3.155	-4.389	-2.500
2.5	.226	.047	-.234	-.482	-.756	-1.032	-1.634	-2.472	-3.161	-2.478
5.0	-.040	-.199	-.401	-.582	-.789	-.992	-1.424	-1.881	-2.378	-2.604
7.5	-.093	-.226	-.395	-.536	-.695	-.844	-1.154	-1.495	-1.880	-2.242
10	------	------	------	------	------	------	------	------	------	------
15	-.186	-.273	-.382	-.476	-.587	-.684	-.924	-1.112	-1.315	-1.810
20	-.246	-.313	-.409	-.496	-.553	-.610	-.790	-.978	-1.126	-1.333
30	-.326	-.386	-.462	-.529	-.560	-.550	-.742	-.964	-.970	-.892
40	-.386	-.439	-.502	-.549	-.574	-.620	-.702	-.716	-.850	-.666
50	-.473	-.512	-.556	-.596	-.628	-.656	-.715	-.777	-.776	-.640
60	-.519	-.552	-.582	-.516	-.628	-.650	-.674	-.704	-.654	-.533
70	-.453	-.473	-.509	-.516	-.486	-.489	-.486	-.469	-.398	-.400
Upper Inner Surface										
1	0.013	0.027	0.060	0.074	0.081	0.087	0.074	0.067	-0.142	-0.027
2.5	.080	.246	.482	.730	.769	.830	.898	.938	.964	.953
5	.226	.652	.850	.851	.863	.878	.918	.878	.870	.832
Lower Surface										
3.2	0.426	0.453	0.516	0.683	0.863	0.958	0.985	0.770	0.344	0.080
4.2	1.340	-1.065	-.743	-.449	-.182	.054	.439	.743	.917	.932
5.7	1.200	-.984	-.737	-.516	-.304	-.107	.216	.482	.694	.752
8.2	-.972	-.818	-.643	-.496	-.344	-.282	.054	.288	.478	.546
10.7	-.758	-.639	-.514	-.402	-.283	-.168	.034	.214	.398	.446
13.2	-.652	-.572	-.449	-.342	-.236	-.147	.020	.167	.317	.393
18.2	-.532	-.459	-.368	-.295	-.203	-.134	0	.114	.243	.306
23.2	-.479	-.426	-.355	-.288	-.209	-.154	-.040	.737	.849	.233
33.2	-.426	-.379	-.348	-.281	-.243	-.209	-.108	-.027	.606	.107
43.2	-.386	-.426	-.315	-.275	-.243	-.214	-.142	-.067	-.007	.033
53.2	-.406	-.380	-.342	-.308	-.284	-.255	-.196	-.134	-.088	-.040
63.2	-.413	-.393	-.368	-.342	-.317	-.302	-.250	-.201	-.155	-.133
73.2	-.246	-.240	-.221	-.208	-.182	-.188	-.175	-.147	-.782	-.100
Lower Inner Surface										
4.2	0.626	0.772	0.870	0.877	0.870	0.858	0.810	0.764	0.654	0.167
5.7	.506	.685	.803	.817	.823	.818	.790	.737	.870	.606

CONFIDENTIAL

NATIONAL ADVISORY COMMITTEE FOR AERONAUTICS

TABLE XI.- DUCT OUTBOARD-CLOSING-SHAPE PRESSURE DISTRIBUTION, 1/4-SCALE FLOW MODEL OF A FIGHTER AIRPLANE

~~CONFIDENTIAL~~

% chord \ α	P								
	-2.02	-1.01	0	1.02	2.05	4.07	6.18	8.13	10.14
Upper surface									
0	0.730	0.886	0.958	0.998	1.000	0.797	0.442	-0.121	-0.895
1.0	.428	.040	-.275	-.778	-1.270	-2.412	-3.740	-5.200	-6.146
7.5	-.129	.379	-.416	-.590	-.740	-1.058	-1.405	-1.755	-2.230
10	-.217	-.358	-.469	-.623	-.774	-1.052	-1.350	-1.641	-2.038
15	-.285	-.398	-.496	-.623	-.734	-.938	-1.167	-1.374	-1.672
30	-.401	-.466	-.522	-.610	-.666	-.777	-.903	-.998	-1.164
Lower surface									
1.0	-.041	.346	.550	.998	.910	.998	.890	.590	1.000
2.5	-.591	-.293	-.121	.100	.279	.576	.781	.904	.881
5	-.598	-.379	-.241	-.054	.095	.362	.564	.724	.730
7.5	-.605	-.413	-.302	-.154	-.027	.214	.401	.563	-.021

~~CONFIDENTIAL~~

NATIONAL ADVISORY COMMITTEE FOR AERONAUTICS

CONFIDENTIAL

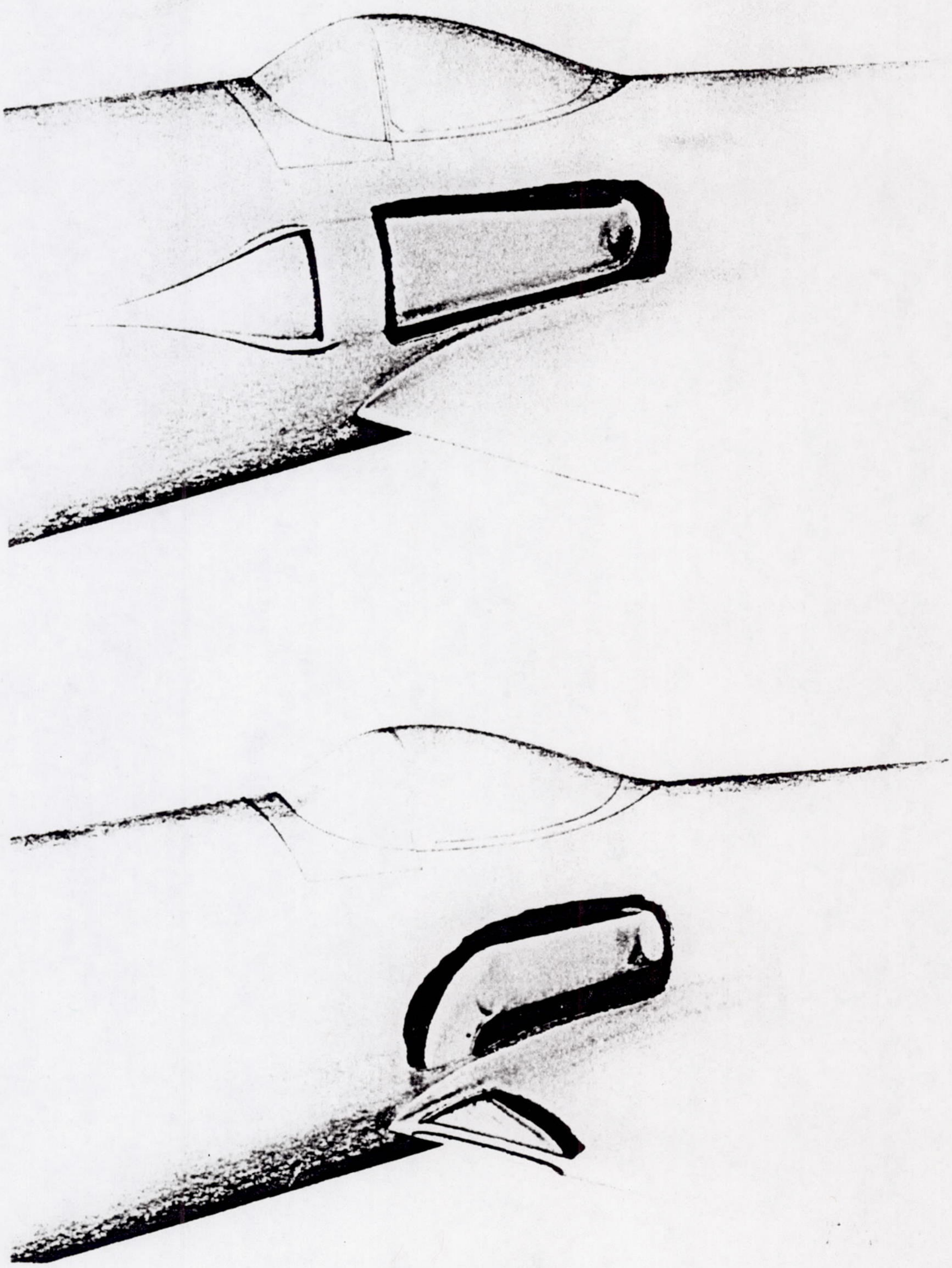

Figure 1.- Comparison of the NACA submerged duct system and the wing leading-edge duct system as applied to the fighter airplane.

CONFIDENTIAL

~~CONFIDENTIAL~~

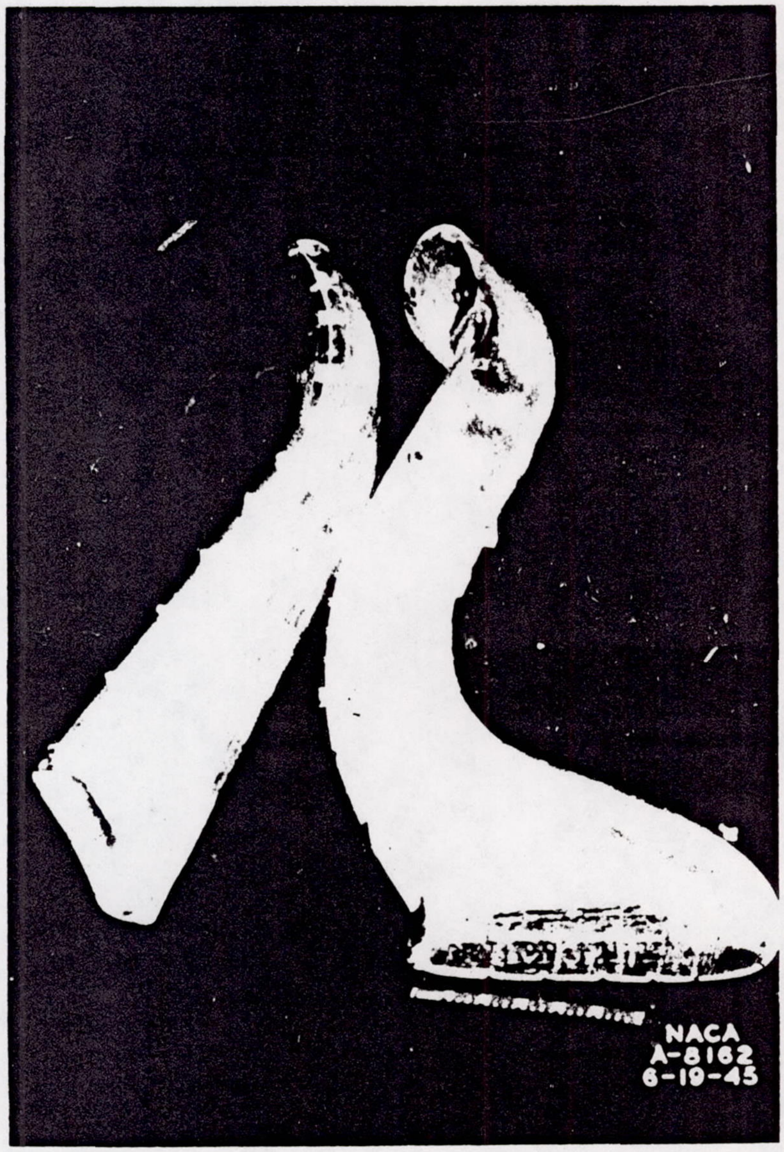

Figure 2.- Comparison of the internal-ducting systems for the NACA submerged duct entry and wing leading-edge duct entry for the $\frac{1}{4}$-scale flow model of the fighter airplane. ~~CONFIDENTIAL~~

~~CONFIDENTIAL~~

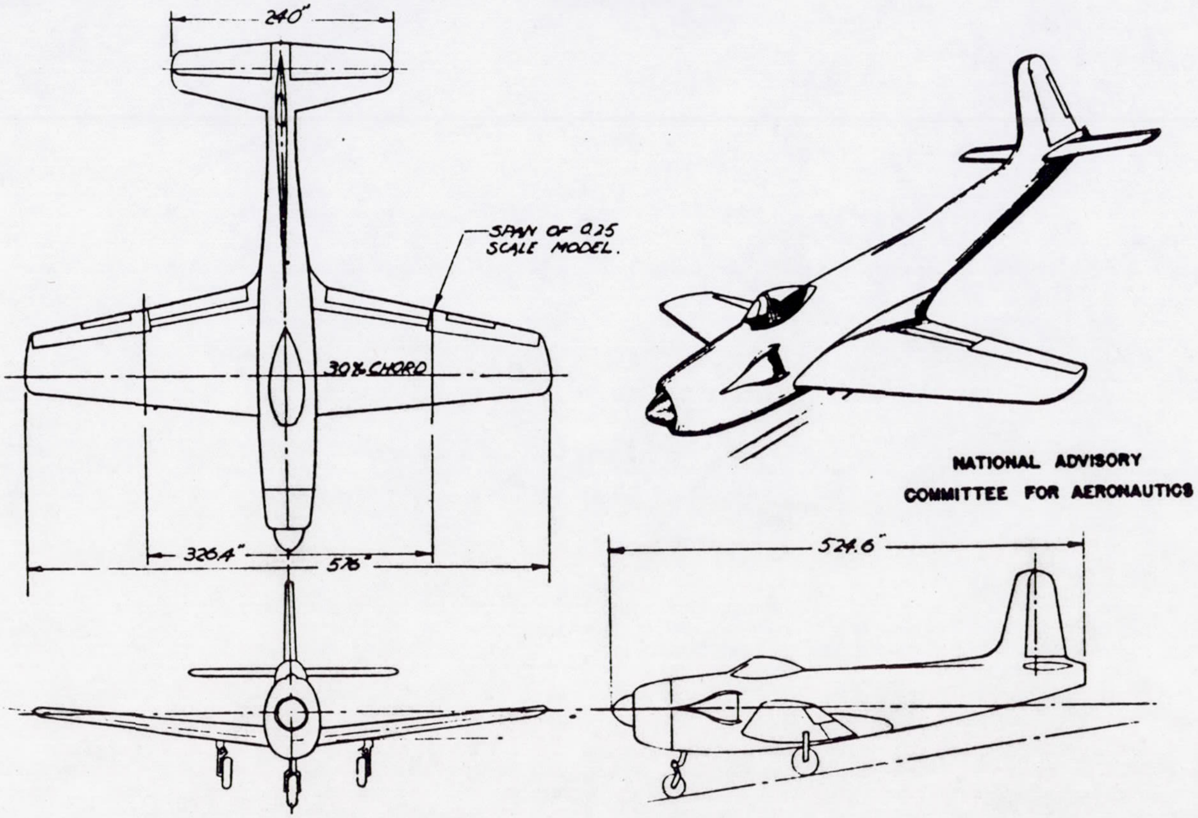

Figure 3.- General arrangement of the fighter airplane equipped with NACA submerged duct entries.

~~CONFIDENTIAL~~

~~CONFIDENTIAL~~

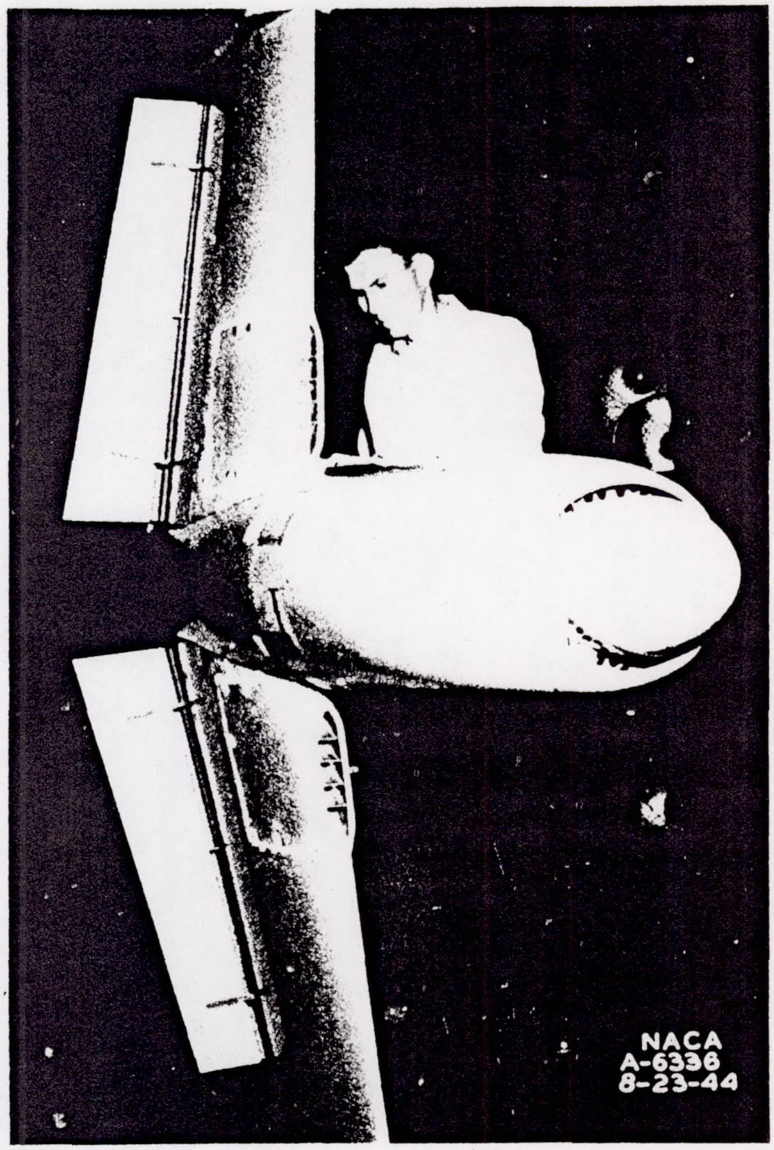

Figure 4.- The $\frac{1}{4}$-scale flow model of the fighter airplane, equipped with wing leading-edge duct entries and the flaps deflected 50°, installed in the Ames 7- by 10-foot wind tunnel No. 1.

~~CONFIDENTIAL~~

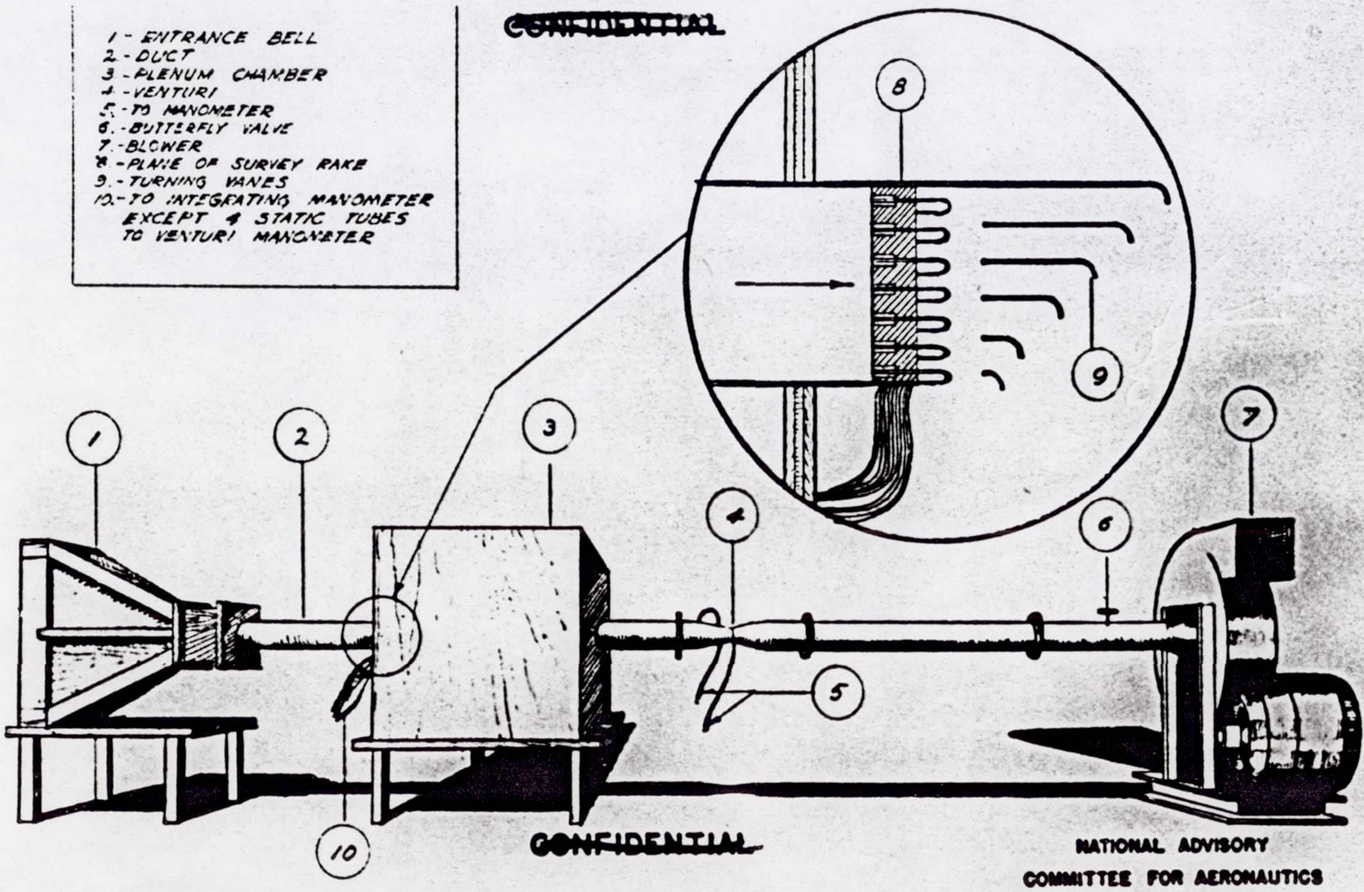

Figure 5.- Schematic view of the test setup for the separate tests of the internal ducting systems for the fighter airplane.

~~CONFIDENTIAL~~

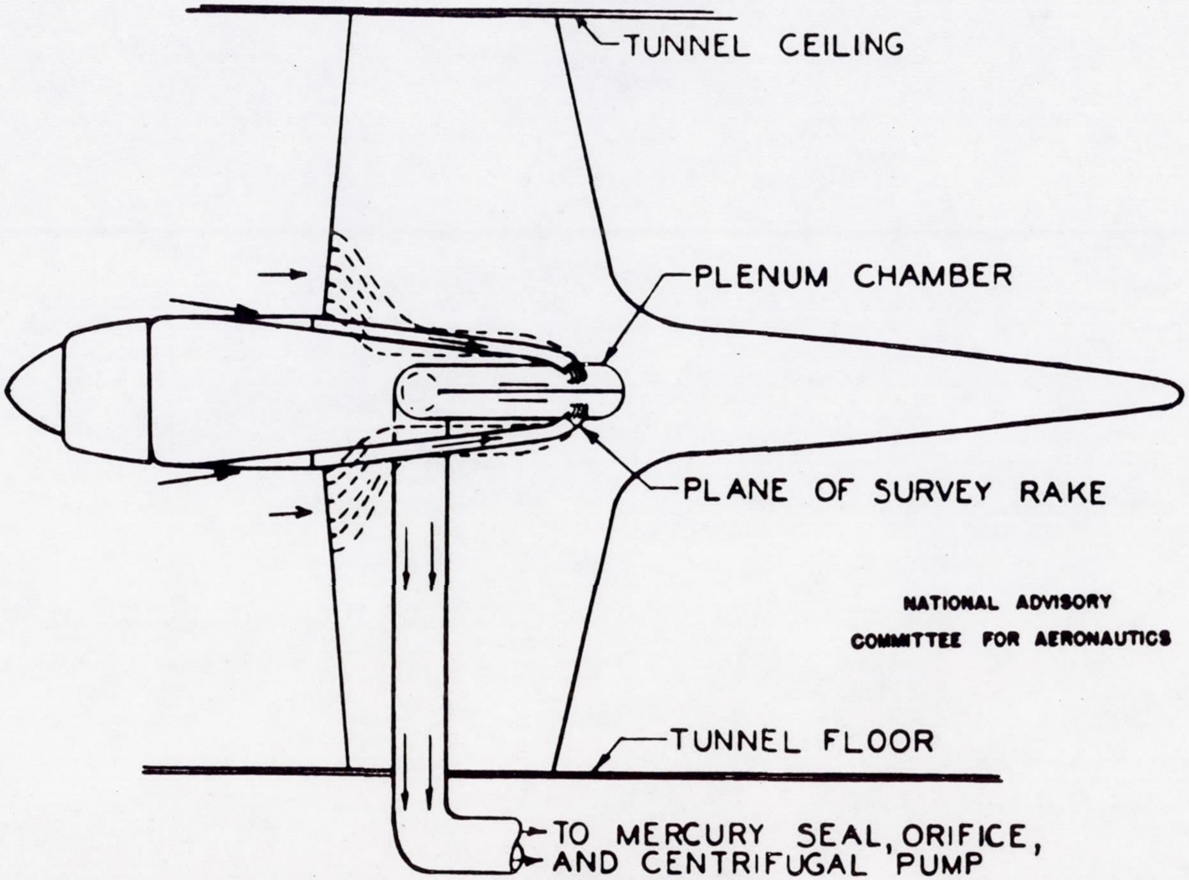

~~CONFIDENTIAL~~

Figure 6.- Internal flow diagram of the $\frac{1}{4}$-scale flow model.

~~CONFIDENTIAL~~

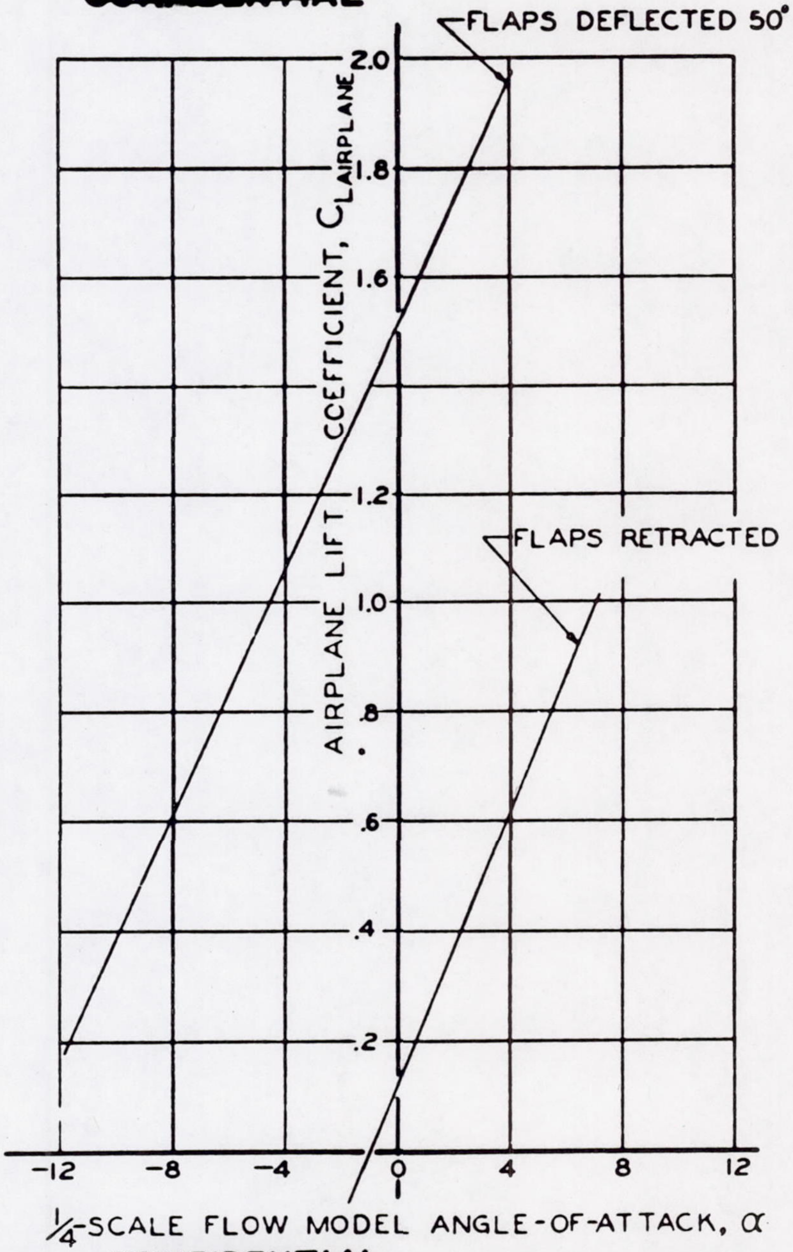

~~CONFIDENTIAL~~

NATIONAL ADVISORY COMMITTEE FOR AERONAUTICS

Figure 7.- Variation of airplane lift coefficient with the $\frac{1}{4}$-scale model angle of attack for the fighter airplane. Gross weight = 16,4000.

~~CONFIDENTIAL~~

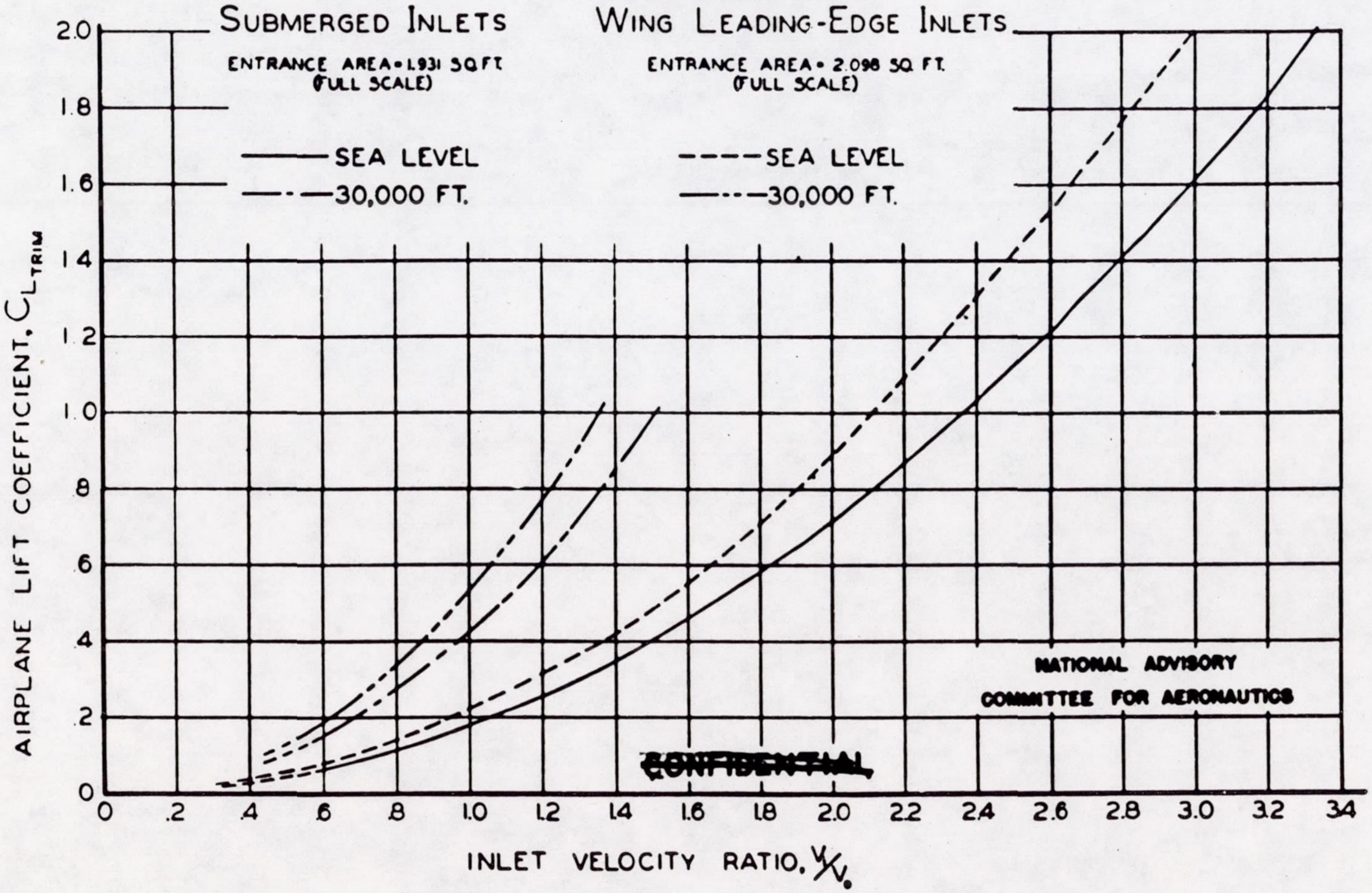

~~CONFIDENTIAL~~

Figure 8.- Variation of airplane lift coefficient with inlet-velocity ratio for 100-percent total-head recovery. Gross weight = 16,400 lb.

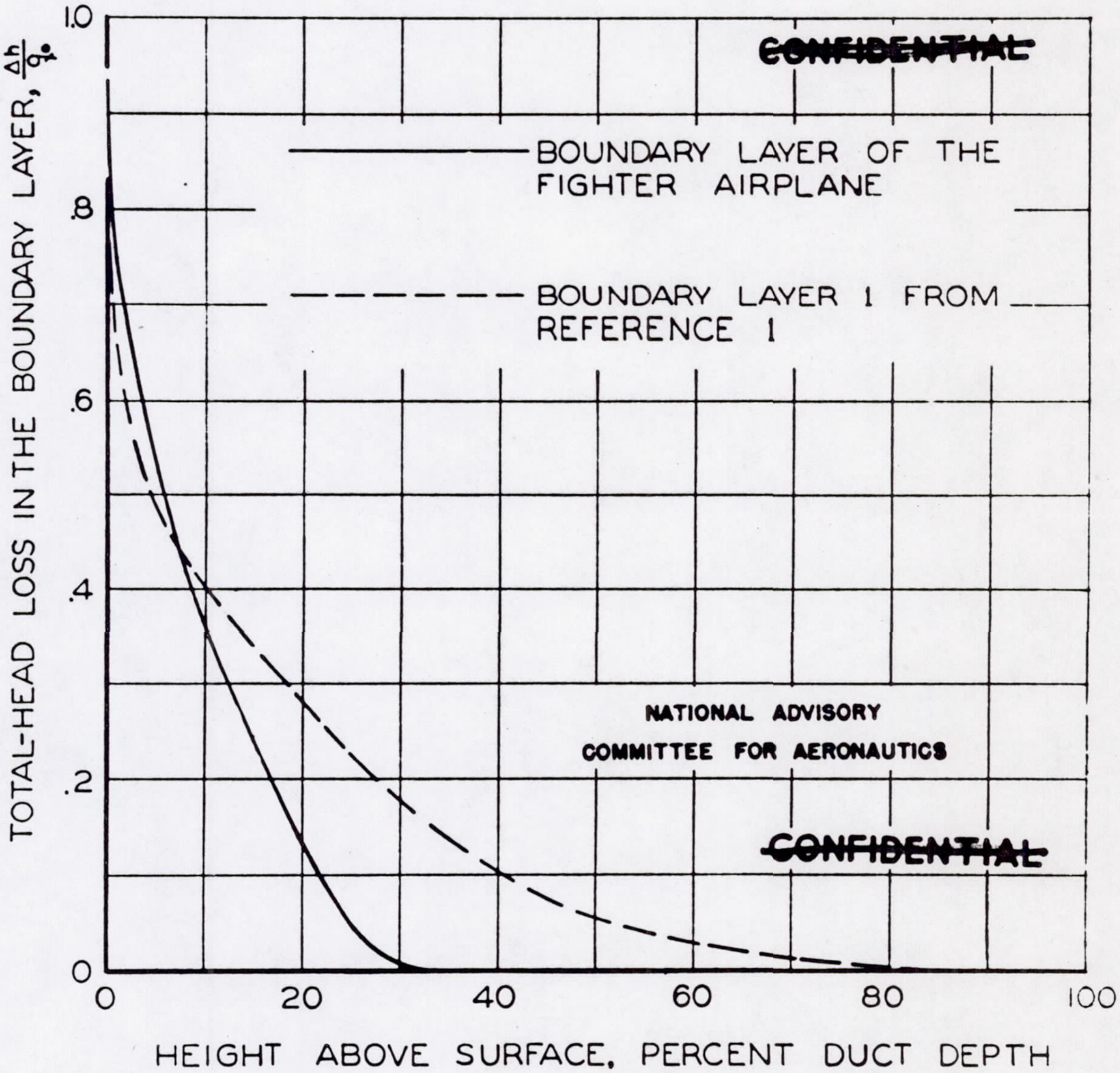

Figure 9.- Comparison of boundary 1 of reference 1 with the boundary layer at entrance to the NACA submerged duct entry for the $\frac{1}{4}$-scale flow model of the fighter airplane.

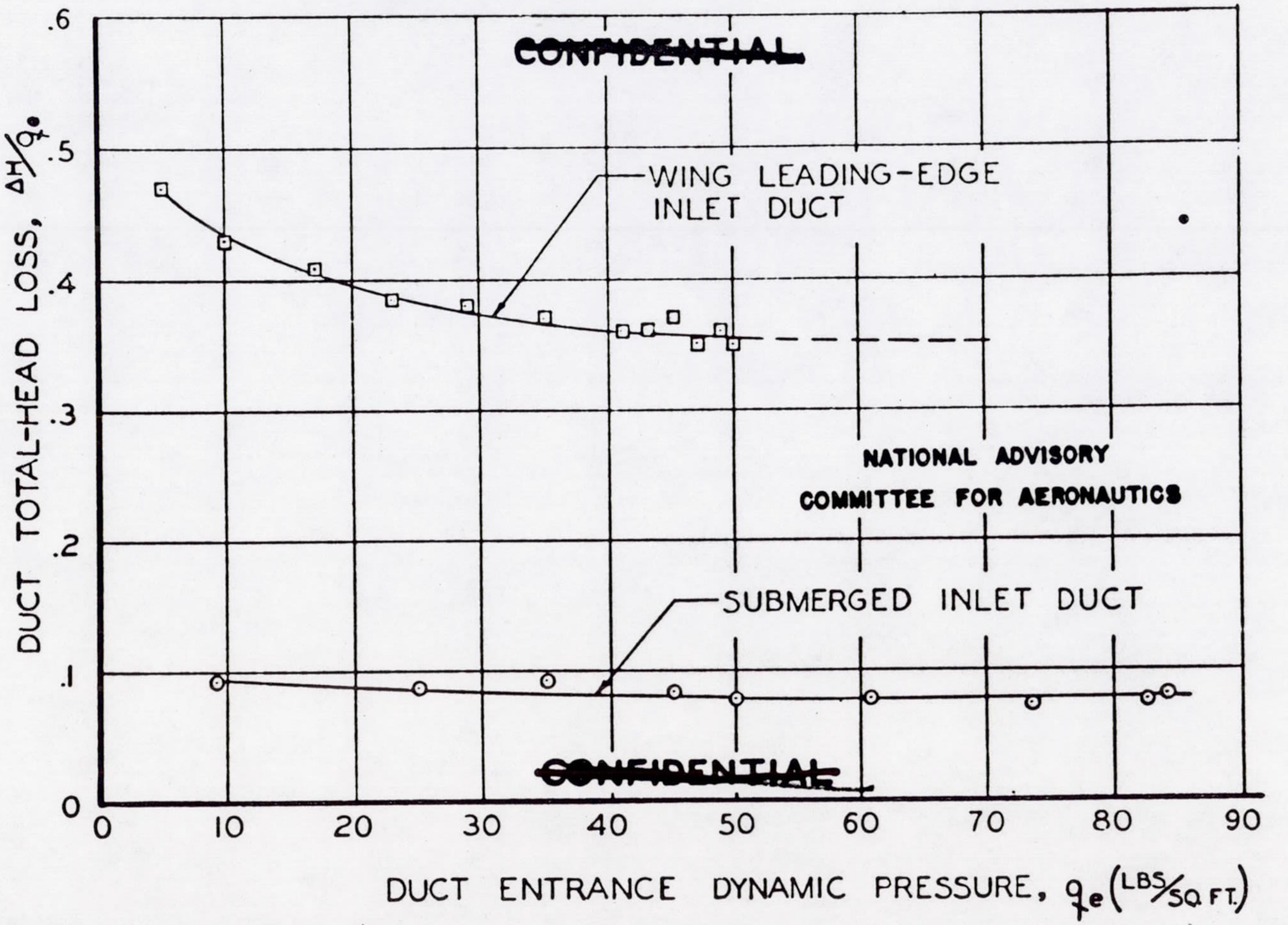

Figure 10.- Variation of total-head loss with duct-entrance dynamic pressure for the internal ducting systems of the $\frac{1}{4}$-scale flow model of the fighter airplane.

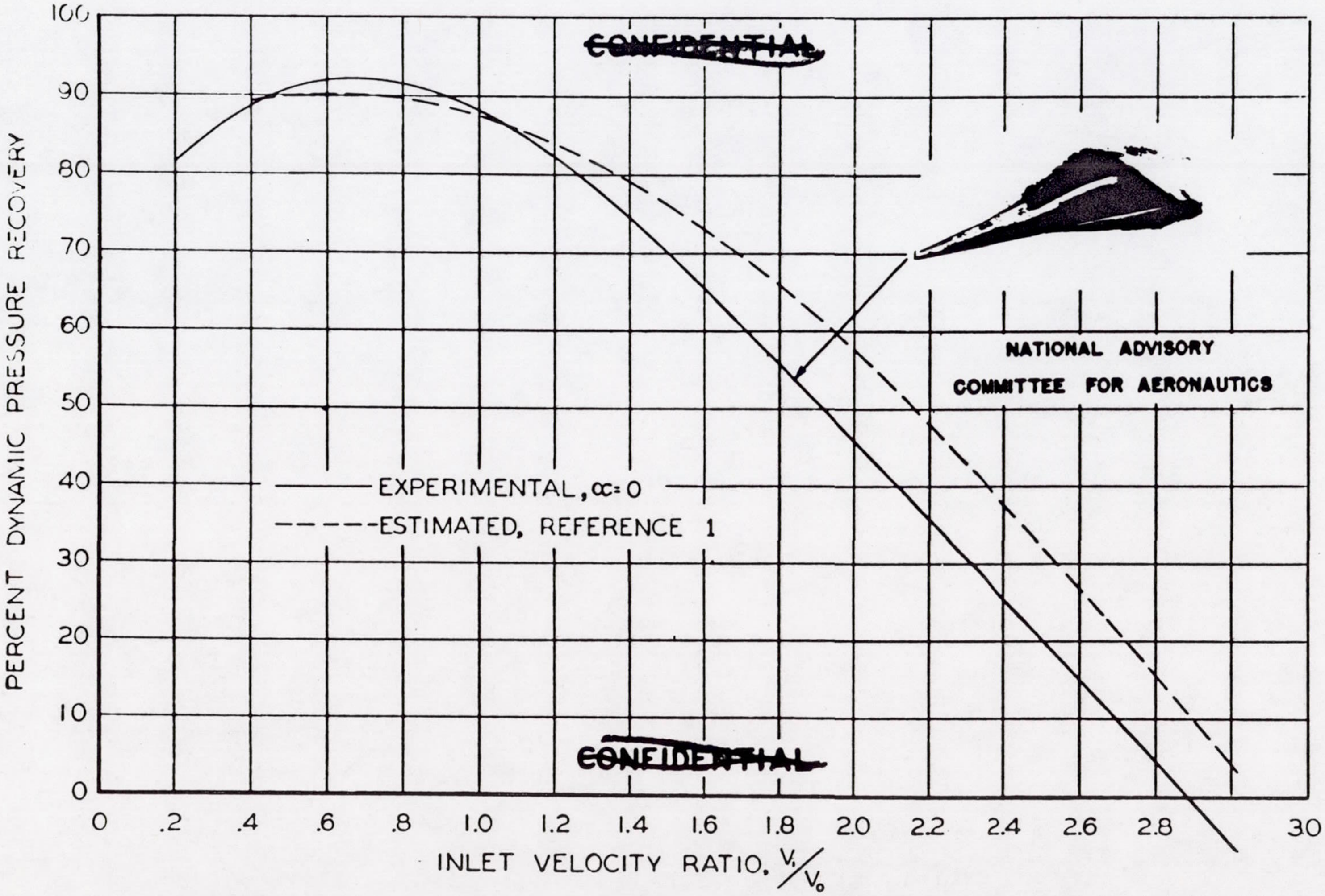

Figure 11.- Comparison of experimental and estimated dynamic pressure recovery for NACA submerged duct entries on a $\frac{1}{4}$-scale flow model of a fighter airplane.

CONFIDENTIAL

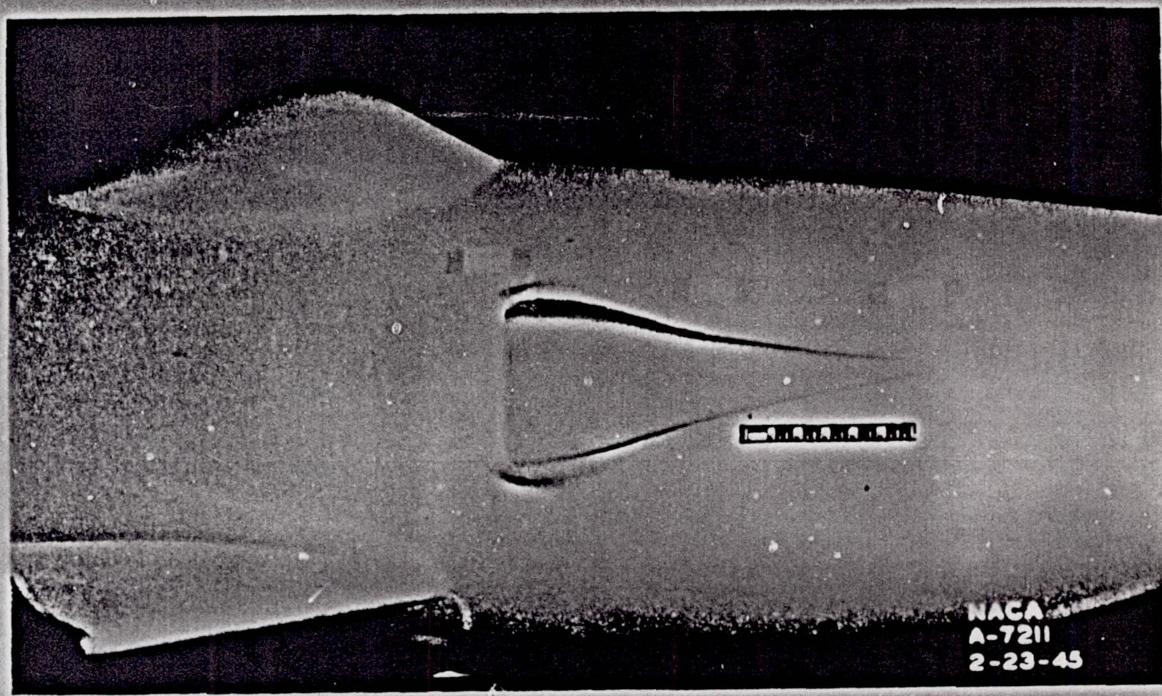

(a) Side view of duct showing station markings on fuselage.

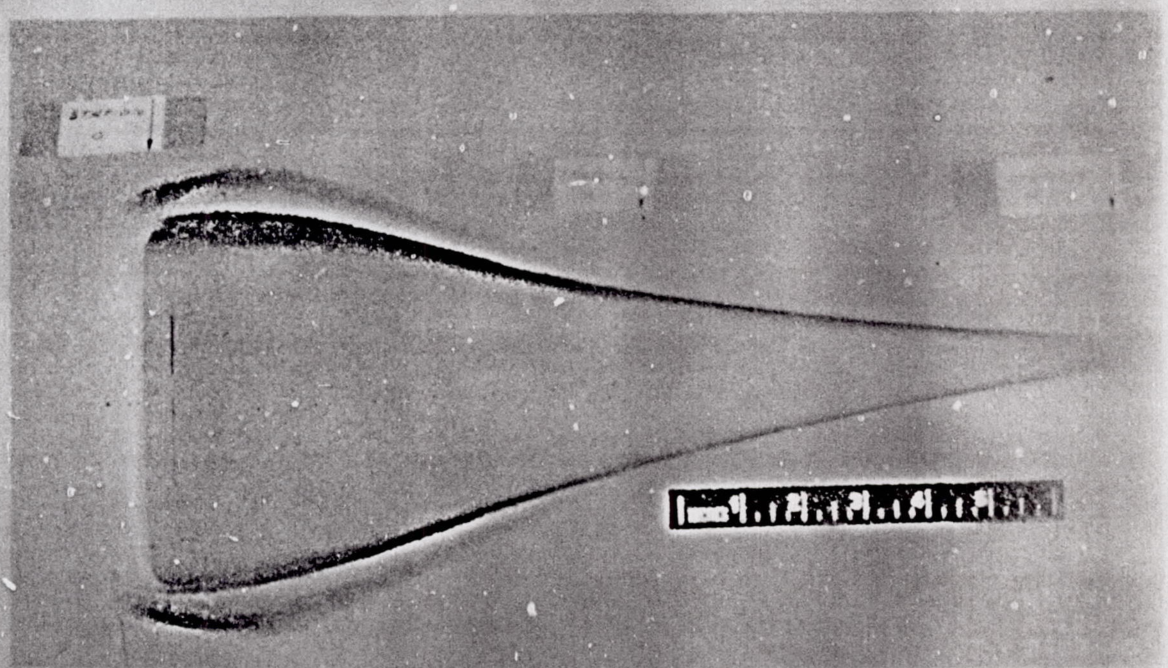

(b) Close-up of duct showing station markings on fuselage.

CONFIDENTIAL

Figure 12.- Views of the final configuration of the NACA submerged

~~CONFIDENTIAL~~

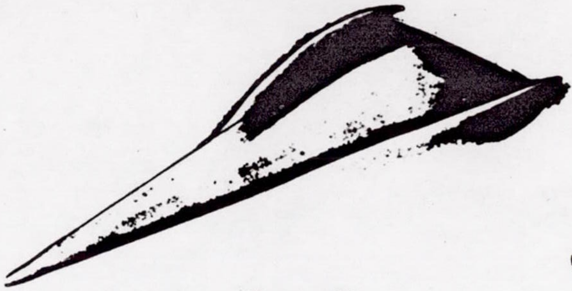

NATIONAL ADVISORY
COMMITTEE FOR AERONAUTICS

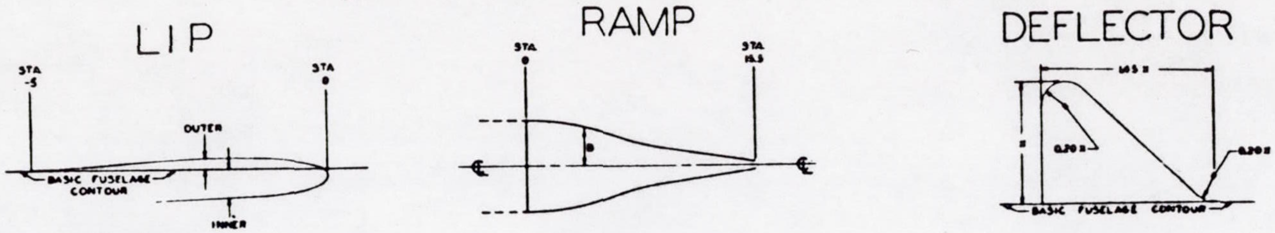

ORDINATES

STATION	INNER	OUTER
0	0.125	RAD-0.125
0.10	0.250	0.010
0.25	0.315	0.060
0.50	0.375	0.115
0.75	0.4[illegible]5	0.145
1.00	0.453	0.160
1.50	0.473	0.170
2.00	1.25" SLOPE	0.170
2.50		0.150
3.00		0.120
3.50		0.085
4.00		0.050
4.50		0.025
5.00		0

ORDINATES

STATION	"B"
0 (LIP)	3.000
1.55	2.965
3.10	2.745
4.65	2.295
6.20	1.845
7.75	1.400
9.30	1.170
10.85	0.940
12.40	0.710
13.95	0.480
15.50	0.250

ALL ORDINATES ARE INCHES, MODEL SCALE.

ORDINATES

STATION	"X"
-0.5	0
-0.25	0.0[illegible]
0 (LIP)	0.21
0.5	0.47
1.0	0.61
1.5	0.[illegible]
2.0	0.70
2.5	0.[illegible]
3.0	0.67
3.5	0.63
4.0	0.5[illegible]
4.5	0.50
5.0	0.44
5.5	0.33
6.0	0.28
6.5	0.20
7.0	0.11
7.5	0.04
8.0	0

~~CONFIDENTIAL~~

Figure 13.- Lip, ramp, and deflector ordinates for the NACA submerged duct entry on the $\frac{1}{4}$-scale flow model of the fighter airplane.

NATIONAL ADVISORY
COMMITTEE FOR AERONAUTICS

BASIC WING, STA. 12.50

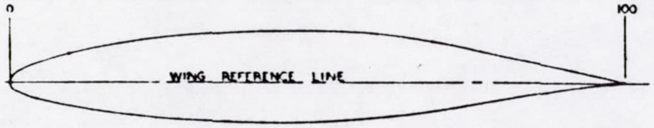

DUCT, STA. 12.50

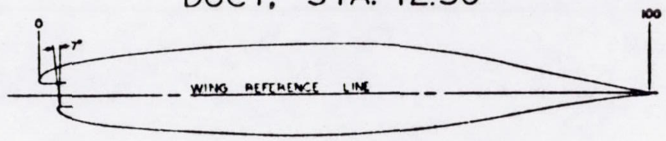

ORDINATES

UPPER SURFACE STA % CHORD	UPPER SURFACE ORD % CHORD	LOWER SURFACE STA % CHORD	LOWER SURFACE ORD % CHORD
0	-0.11	0	-0.11
0.49	1.05	0.50	-1.06
0.74	1.27	0.75	-1.21
1.24	1.59	1.25	-1.48
2.49	2.21	2.51	-1.95
4.99	3.31	5.01	-2.51
7.49	3.88	7.51	-3.13
9.98	4.52	10.01	-3.56
14.98	5.54	15.01	-4.26
19.98	6.33	20.01	-4.77
24.98	6.95	25.02	-5.17
30.00	7.44	30.00	-5.47
34.97	7.77	35.02	-5.67
39.97	7.99	40.02	-5.78
44.97	8.11	45.02	-5.80
49.98	8.06	50.02	-5.73
54.97	7.9[illegible]	55.02	-5.52
59.98	[illegible]	60.02	-5.22
64.98	7.04	65.0[illegible]	-4.71
70.00	6.25	70.00	-3.99
74.99	5.3[illegible]	75.01	-3.18
79.99	4.32	80.01	-2.35
84.99	3.32	85.00	-1.57
89.99	2.32	90.00	-0.83
94.99	1.32	95.00	-0.20
100.00	0.31	100.00	0.19

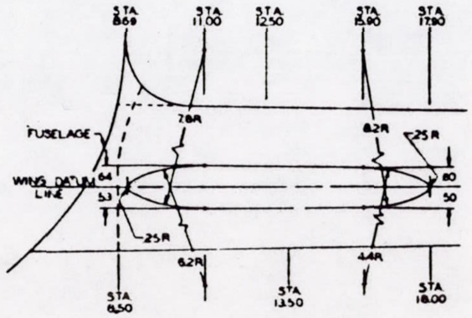

DUCT OPENING AT
ANGLE 7°

DIMENSIONS ARE INCHES, MODEL SCALE
RADII ARE APPROXIMATE

ORDINATES

STA. % CHORD	OUTER SURFACES UPPER % CHORD	OUTER SURFACES LOWER % CHORD	INNER SURFACES UPPER % CHORD	INNER SURFACES LOWER % CHORD
0	2.38	—	2.38	—
0.2	2.84	—	1.93	—
0.5	3.16	—	1.85	—
1.0	3.49	—	1.85	—
2.0	3.95	—	1.92	—
3.17	4.38	-1.97	2.01	-1.97
3.3	—	-2.29	—	-1.71
3.5	—	-2.46	—	-1.65
3.75	—	-2.64	—	-1.63
4.0	4.62	-2.79	2.06	-1.61
4.76	—	—	2.13	—
5.0	4.87	-3.21	—	—
6.34	5.15	-3.63	—	—
7.5	5.38	-3.89	—	—
10.0	5.74	-4.31	—	—
15.0	6.34	-4.74	—	—
20.0	6.85	-5.08	—	—
30.0	7.61	-5.59	—	—
40.0	7.99	-5.78	—	—
45.0	8.11	-5.80	—	—
50.0	8.08	-5.73	—	—
60.0	7.58	-5.22	—	—
100.0	SAME AS BASIC WING			
L.E. RADII: 0.32 % CHORD				

Figure 14.- Detail sketch and ordinates of the wing leading edge inlet for the $\frac{1}{4}$-scale flow model of the fighter airplane.

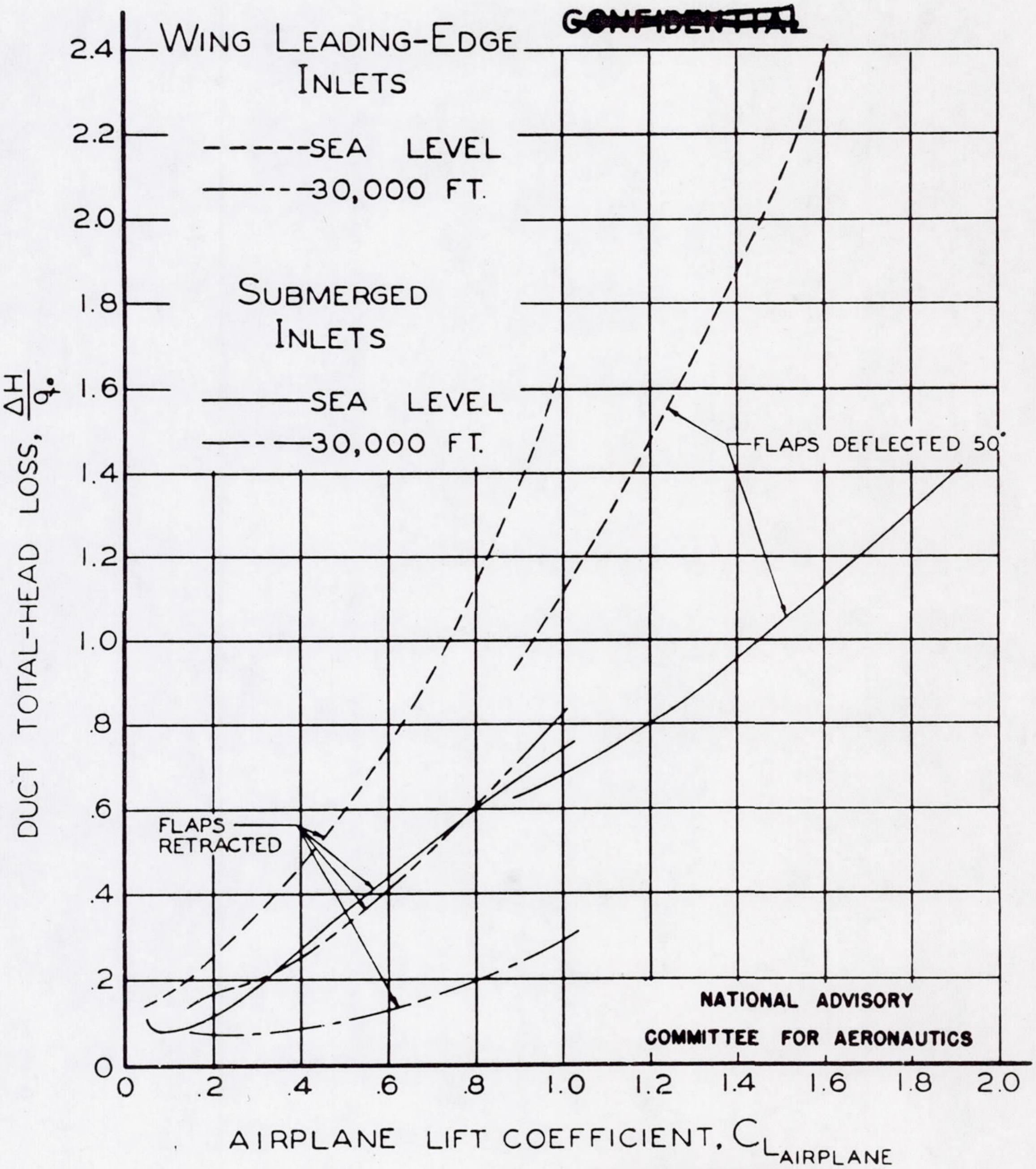

Figure 15.- Comparison of the duct system losses at the simulated compressor entrance for the $\frac{1}{4}$-scale flow model of the fighter airplane.

~~CONFIDENTIAL~~

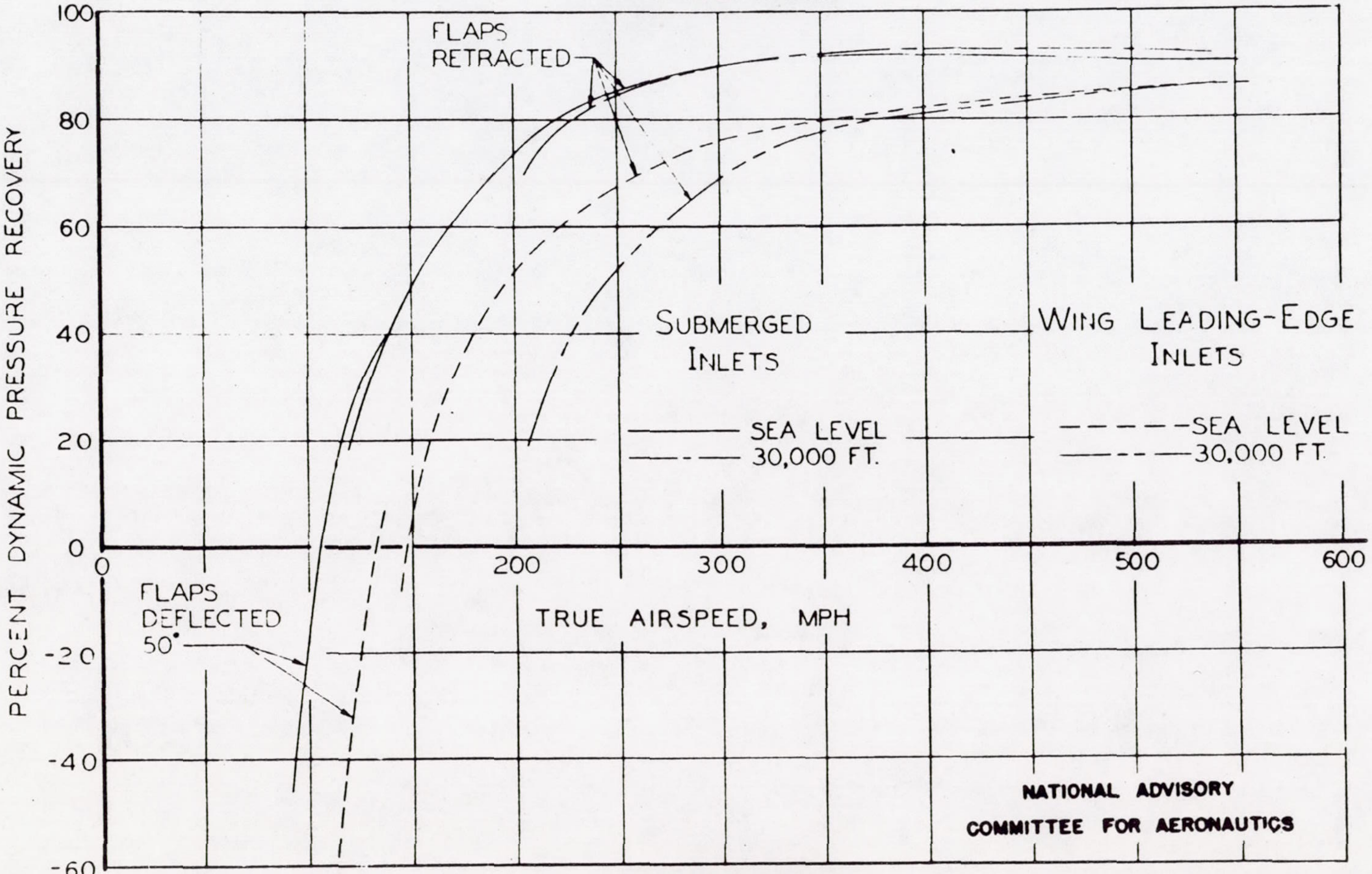

~~CONFIDENTIAL~~

Figure 16.- Comparison of dynamic pressure recovery for the wing duct entry and NACA submerged duct entry for the fighter airplane.

~~CONFIDENTIAL~~

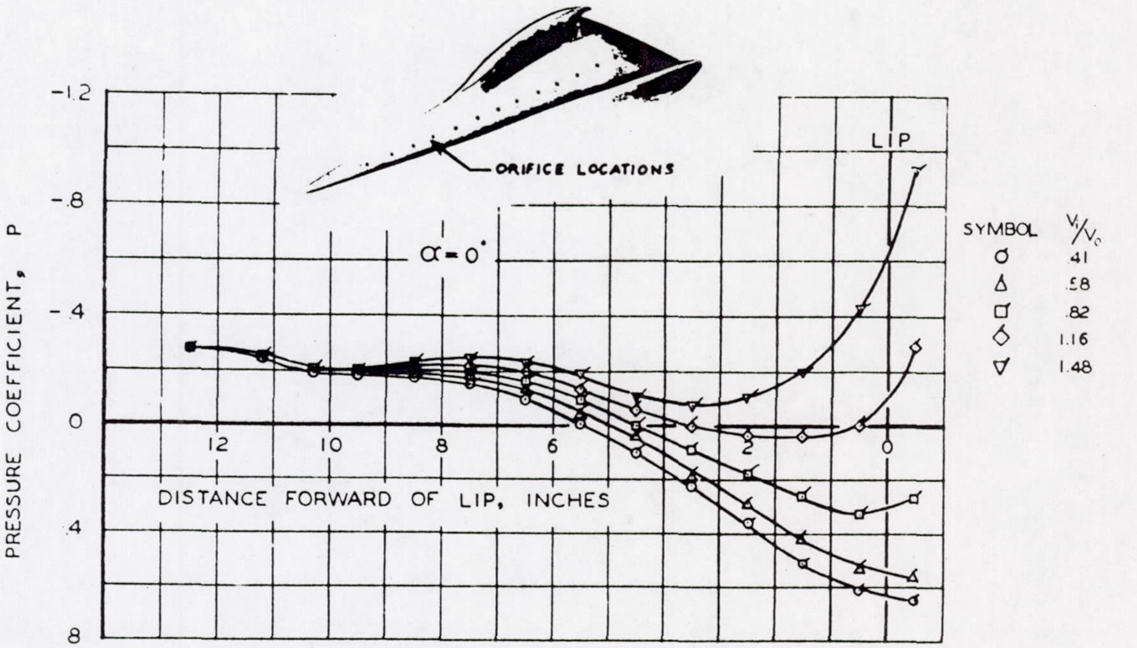

NATIONAL ADVISORY
COMMITTEE FOR AERONAUTICS

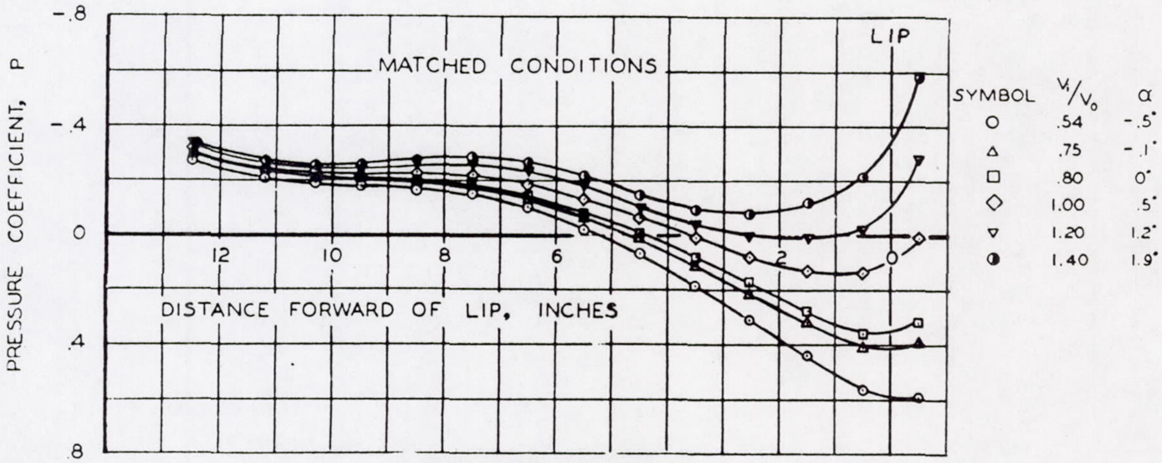

~~CONFIDENTIAL~~

Figure 17.- Pressure distribution along the ramp of the $\frac{1}{4}$-scale flow model of the fighter airplane.

~~CONFIDENTIAL~~

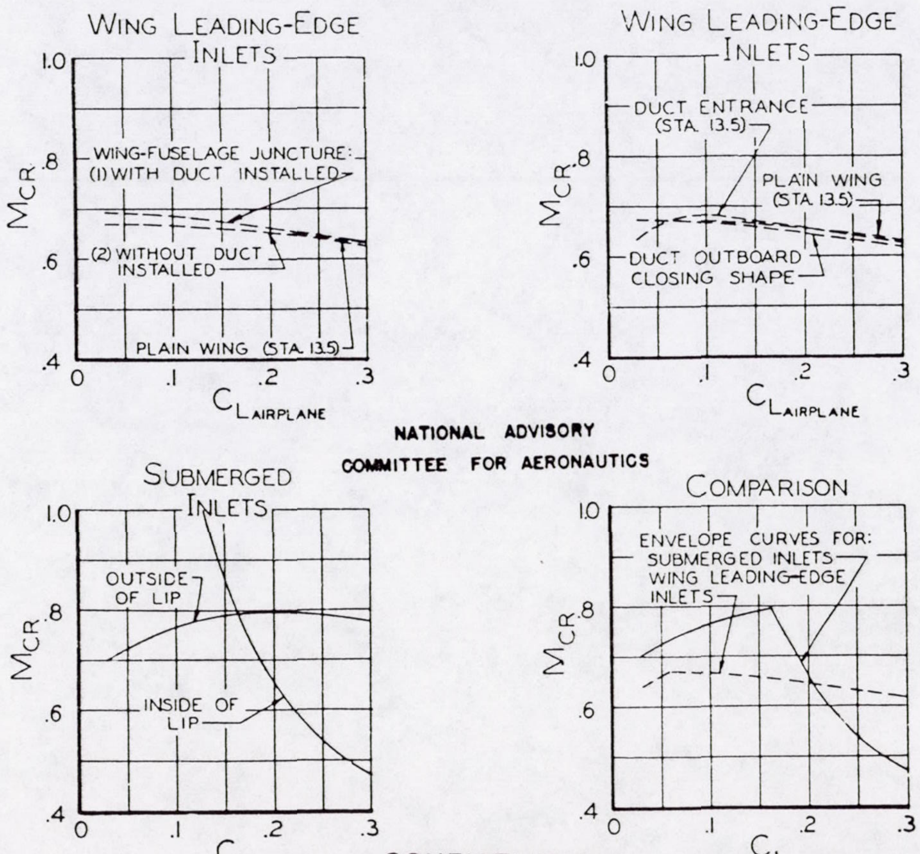

~~CONFIDENTIAL~~

Figure 18.- Critical Mach number at matched sea level flight conditions for the NACA submerged inlet and the wing leading-edge inlet on the $\frac{1}{4}$-scale flow model of a fighter airplane.